

1 **Understanding hydroclimate processes in the Murray-Darling**
2 **Basin for natural resources management**

3
4 Ailie J. E. Gallant¹, Anthony S. Kiem², Danielle C. Verdon-Kidd², Roger C.
5 Stone³, David J. Karoly¹

6
7 ¹ School of Earth Sciences, University of Melbourne, Parkville, VIC, 3010,
8 Australia

9 ² Environmental and Climate Change Research Group, School of
10 Environmental and Life Sciences, University of Newcastle, Callaghan, NSW, 2308,
11 Australia

12 ³ Australian Centre for Sustainable Catchments, University of Southern
13 Queensland, Toowoomba, QLD, 4350, Australia

14
15 **Corresponding author:**

16 Dr Ailie Gallant

17 School of Earth Sciences, University of Melbourne, Parkville, VIC, 3010

18 Phone: +61 3 8344 7304

19 Email: agallant@unimelb.edu.au

21 **Abstract**

22 Isolating the causes of extreme variations or changes in the hydroclimate is
23 difficult due to the complexities of the driving mechanisms, but it is crucial for
24 effective natural resource management. In Australia's Murray-Darling Basin (MDB),
25 ocean-atmosphere processes causing hydroclimatic variations occur on time scales
26 from days to centuries, all are important, and none are likely to act in isolation.
27 Instead, interactions between all hydroclimatic drivers, on multiple time scales, are
28 likely to have caused the variations observed in MDB instrumental records. A
29 simplified framework is presented to assist natural resource managers in identifying
30 the potential causes of a hydroclimatic event. The framework condenses an event into
31 its fundamental elements, including its spatial and temporal signal and small-scale
32 evolution. The climatic processes that are potentially responsible for the event are
33 then examined to determine possible causes. The framework was applied to an event
34 occurring from 1997–2010 when the southern MDB experienced prolonged and
35 severe dry conditions, providing insights into possible causal mechanisms that are
36 consistent with recent studies. The framework also assists in identifying uncertainties
37 and gaps in our understanding that need to be addressed.

38

1. Introduction

Periods of prolonged, severe drought and moisture surplus are challenging for natural resources management/managers (NRM). The events that are at the very edge of past experience are of particular concern as they push the limits upon which standard management practices are based, making socioeconomic and some natural systems vulnerable. The unprecedented impacts of these extreme events can sometimes necessarily force a somewhat *ad hoc* management response, which may be successful but may also lead to undesirable outcomes (i.e. maladaptation). Recent periods of prolonged wet and dry conditions have provided further cause for thought as NRM debate the causes of these extreme conditions, whether they are linked to anthropogenic climate change, whether similar events may become more prevalent in the future, and even whether such periods should be considered the new norm.

Several extreme climatic events have recently occurred in Australia's largest food-producing region, the Murray–Darling Basin (MDB). Much of the region experienced ongoing drought from around late-1996 to mid-2010 [Murphy and Timbal, 2008], which was followed by a rapid transition to extremely wet conditions across the MDB, the north in particular, from late 2010 to the time of publication of this article. Management practices were tested throughout the sometimes-unprecedented nature of both periods and there were several instances when water resource managers, agriculturalists and biodiversity managers (hereafter collectively referred to as NRM) increasingly questioned whether the conditions in parts of the MDB contained an anthropogenic component.

61 To understand the causes of the recent changes to the MDB climate, and
62 potential future changes that include the effects of anthropogenic climate change,
63 several national research initiatives were established. These initiatives included the
64 Murray Darling-Basin Sustainable Yields Project (MDBSY;
65 www.csiro.au/partnerships/MDBSY); the South Eastern Australian Climate Initiative
66 (SEACI; www.mdbc.gov.au/subs/seaci); the Indian Ocean Climate Initiative (IOCI;
67 www.ioci.org.au); and the CSIRO-BoM Climate Change in Australia project
68 (www.climatechangeinaustralia.gov.au). The collective research from these, and
69 other, initiatives has provided invaluable information that is highly relevant to the
70 NRM community.

71 However, increasing the body of knowledge has the potential to be confusing
72 for NRM. For example, the climate science community has identified a number of
73 physical processes that influence variations in the MDB hydroclimate, which are often
74 relayed to the NRM community as climate indices (i.e. simplified metrics of these
75 atmosphere-ocean processes). Unavoidably, the number of these indices, and opinions
76 as to what is important and what is not, increases as more research is conducted,
77 adding uncertainty and complicating the information for those relying on it for risk
78 assessment.

79 Given the difficulties NRM might have utilizing the large amount of climate
80 information available, this paper has two primary objectives. The first is to synthesize
81 knowledge about the processes governing climatic variations across the MDB. This
82 synthesis will distil up-to-date information in a concise form so that it may be
83 interpreted more easily than compiling information from self-guided literature
84 surveys. *Murphy and Timbal* [2008] have previously presented a synthesis of the

85 major processes driving inter-annual and shorter time scale climatic variations in
86 southeast Australia. While useful for the southern MDB, *Murphy and Timbal's* [2008]
87 paper did not describe the importance of these and other climate processes for the
88 northern MDB. Furthermore, information on decadal and longer-scale climate
89 processes, interactions between climate drivers and interactions between climate and
90 hydrological processes were not included in their review but are highly relevant for
91 NRM in the MDB.

92 The second objective is to identify a broad framework that allows NRM to
93 scrutinize existing climate knowledge in order to better isolate the potential
94 cause/causes of a climatic event. It is hoped this may make information relating to
95 hydroclimatic processes more useful in risk management applications. Such a
96 framework simplifies a complex problem and so inherently includes a large degree of
97 uncertainty as it is derived from a mostly chaotic system. So, while the framework
98 does not provide absolute answers, we argue that it establishes a more focused set of
99 considerations for NRM. Furthermore, the framework highlights areas where the
100 knowledge base is lacking (i.e. areas with large uncertainty or actual knowledge
101 gaps), thus identifying areas of future research that, if undertaken, will also prove
102 useful for NRM.

103 To fulfil these objectives, the paper is presented as follows: first, a
104 hydroclimatology for the MDB provides context. The synthesis on climate processes
105 is then presented. This includes describing processes acting on inter-annual and
106 shorter scales as an update *Murphy and Timbal* [2008] and an explanation on the
107 drivers of decadal and longer-scale variability, which has not previously been
108 presented. We then show analysis for an emerging area of the science that, we argue,

is critical to understanding and predicting wet and dry cycles in the MDB, namely interactions between climate processes. Finally, the framework for highlighting the potential cause/causes of climatic events for NRM is presented and applied to the case of the prolonged drought that affected the southern MDB for over 13 years from the mid 1990s.

2. Hydroclimatology of the Murray-Darling Basin: 1900–2010

The range of hydroclimatic variability on which NRM practices are based has traditionally been defined using historical data. By global standards the climate records in the MDB are long, spanning 111 years from 1900–2010 with some individual stations going back to the mid-1800s. Here, we give an up-to-date overview of the hydroclimatology of the MDB based on these instrumental observations.

Spanning from the subtropics (24°S) to the middle latitudes (38°S), approximately 90% of the MDB is classified as either arid or semi-arid [Maheshwari *et al.*, 1995]. The topography of the Basin consists mostly of extensive plains and low undulating areas, with much of the Basin less than 200 metres above sea level. The landscape varies throughout the catchment from the sub-tropical rainforests of the eastern uplands, to the temperate, sub-alpine regions of the southeast and the hot, dry semi-arid plains in the west [Barros and Bowden, 2008].

Annual rainfall averaged across the MDB is approximately 470 mm per year (calculated over the period 1900 – 2010). However, the spatial variations in annual mean rainfall across the MDB are large (Figure 1). Rainfall is highest in mountainous

areas in the southeast where the mean annual totals can exceed 1500 mm, and lowest in the west of the Basin where they are typically less than 300 mm/year. Averaged across the Basin, evaporation (estimated using pan evaporation) is approximately four times the annual mean rainfall. Geographically, evaporation ranges from approximately 1200 mm/year in the southeast of the Basin to around 2400 mm/year in the west [BoM, 2010].

Over the 111 years from 1900–2010, MDB rainfall has exhibited large inter-annual to multi-decadal fluctuations (Figure 2). Averaged across the MDB, conditions were broadly drier during the first half of the 20th Century with Basin-averaged rainfall deficits frequently exceeding 100 mm/year, equivalent to rainfall being at least 20% below average (Figure 2). Several periods of multi-year rainfall deficits occurred, including the “Federation Drought” (c.1895 – 1902) and the “World War II Drought” (c.1937 – 1945) [Ummenhofer *et al.*, 2009b; Verdon-Kidd and Kiem, 2009b]. Though 19 years in the instrumental record had above average rainfall during the first half of the 20th century (Figure 2), there was only one multi-year wet period prior to 1950 (i.e. 1916 to 1917 when MDB rainfall was at least 20% above average).

The period from 1950 to 2010 was dominated by large decadal-scale variations in rainfall. Two distinct periods during the 1950s and the 1970s had several years with rainfall considerably greater than average and major floods occurred during 1952, 1956 and 1974. Multi-year periods with below average annual rainfall marked the 1960s, early 1980s, and mid-1990s to early 2010. However, there were also some notable floods during these dry epochs, for example, 1990 across much of eastern Australia and more recently 2008 and 2009 in the northern MDB.

The dry conditions from the mid-1990s to early 2010 were dubbed ‘The Big Dry’ or the ‘Millennium Drought’ (hereafter referred to as ‘The Big Dry’ only) [Ummenhofer *et al.*, 2009b; Verdon-Kidd and Kiem, 2009b] (Figure 3). This drought was mainly confined to the southern MDB and was dominated by autumn and early winter rainfall deficits stemming from both a decrease in the number of rain days and a reduction in the intensity of daily rainfall events [Verdon-Kidd and Kiem, 2009b]. The drought was broken in spectacular fashion in 2010, which was the wettest year on record averaged across the MDB. Much of this stemmed from late winter and spring rainfall, which led to annual rainfall being 70% above average (Figure 2).

3. Hydroclimate processes of the Murray-Darling Basin

We direct readers to the review paper by *Murphy and Timbal* [2008] for a broad overview of the key processes relevant to climate variations in the southern MDB on inter-annual and shorter time scales, including the mechanisms by which they occur and their climatological characteristics (e.g. frequency, persistence etc.). Here, we expand on these topics and include information relevant to the northern MDB and interactions between hydroclimate driving mechanisms that are relevant to the whole MDB. The northern and southern MDB are defined as the halves of the Basin north and south of 33°S. To date, less focus has been given to understanding climate processes in the northern MDB by the climate science community and a synthesis has not previously been presented. An explicit discussion of relevant daily-scale processes, a synthesis of the most recent findings on inter and intra-annual processes since *Murphy and Timbal* [2008] was published, and a discussion on the

inter-decadal processes, which has not previously been presented for the MDB are provided.

3.1 Daily to intra-annual processes

The types of weather systems that produce and inhibit rainfall in the MDB are summarized in Figure 4. The origins of these systems vary regionally with the most distinct differences occurring from north to south. The importance of a particular type of weather system to seasonal rainfall totals is heavily dependent on the location. There can be substantial differences in the relative contributions from particular weather systems to seasonal accumulations over distances of several hundred kilometres only [Verdon-Kidd and Kiem, 2009a].

The rainfall accumulations associated with different occurrences of the same type of weather system also vary, and there are differences in the relative amount of rainfall each type of system tends to produce [Pook *et al.*, 2006]. For example, tropical cyclones are more likely to produce higher rainfall totals in the northern MDB compared to frontal systems in the southern MDB. The typical amount of rainfall produced depends on the intensity and duration of each system. Their contribution to the climate depends on those factors and also on the frequency at which those systems impact on an area.

The make up of the daily-scale rainfall distribution is particularly important for water resources management. For example, the impact of a one-month rainfall total of 100 mm on a hydrological system would be very different depending on whether the rainfall had fallen evenly throughout the month, or in a single event [McIntosh *et al.*, 2007; Verdon-Kidd and Kiem, 2009b].

Rainfall in the southern MDB mostly stems from extra-tropical weather systems [Wright, 1989; Qi *et al.*, 1999; Pook *et al.*, 2006; Risbey *et al.*, 2008]. Figure 4 illustrates some of these systems, such as cold fronts, cut-off low-pressure systems and cloud bands. Cut-off low pressure systems contribute the most rainfall from a single type of system, between approximately 25% and 50% of rainfall to the region [Wright, 1989; Pook *et al.*, 2006]. Cut-off lows are also responsible for over 80% of the rainfall that occurs on heavy rain days (described as days with over 25 mm or rain) during these months [Pook *et al.*, 2006].

Frontal systems that interact with tropical air masses (e.g. cloud bands that form from a surface or middle troposphere pressure trough entraining tropical moisture, such as the Northwest cloud band in Figure 4), those that do not (e.g. the cold fronts in Figure 4), and post-frontal rainfall provide smaller, but significant, contributions to southern MDB rainfall totals, although the influence of each varies regionally [Wright, 1989; Verdon-Kidd and Kiem, 2009a]. Post-frontal rainfall is only a significant contributor close to the mountain range spanning the southeast MDB, where orographic uplift is the primary mechanism causing rainfall. In the southern MDB, frontal rain contributes between 25% and 40% of monthly rainfall totals, with this contribution decreasing moving further north [Pook *et al.*, 2006]. Verdon-Kidd and Kiem [2009a] attribute sizeable proportions of rainfall in the state of Victoria in the southern MDB to systems such as pre-frontal and inland troughs that produce cloud bands. However, Wright [1997] and Pook *et al.* [2006] state that such systems are generally responsible for less than 10% of total rainfall in this region.

In the northern MDB, rainfall mostly stems from tropical systems, or from interactions between tropical and extra-tropical systems [Wright, 1997; Sturman and

225 *Tapper*, 2005]. Meridional troughs that extend through the subtropics of eastern
226 Australia, sometimes called ‘easterly-dips’ (Figure 4), can be associated with
227 widespread rain via cloud bands, particularly from April to October. Cloud bands that
228 are initiated from convergence caused by the trough alone account for some 25-40%
229 of rainfall in the northern half of the MDB [*Wright*, 1997]. There is a similar
230 contribution from the interaction between these tropical cloud bands with extra-
231 tropical features such as cold fronts [*Wright*, 1997].

232 Strong cold fronts can penetrate as far north as the Australian tropics. When
233 they occur during the onset and breakdown of the northern wet season (approximately
234 November – March), they may trigger thunderstorms along their leading edge,
235 bringing very localized, heavy rain to areas in the northern MDB [*Sturman and*
236 *Tapper*, 2005]. From December – April, tropical cyclones that have moved inland
237 from the east Australian coast can occasionally contribute large rainfall totals to the
238 northern MDB.

239 High-pressure systems are the features that primarily inhibit rainfall [*Sturman*
240 *and Tapper*, 2005]. Over the MDB, these may constitute part of the climatological
241 belt of high-pressure, known as the sub-tropical ridge (STR), or be independent of it.
242 Persistent and stationary high-pressure systems that are removed from the STR are
243 responsible for the phenomenon of atmospheric blocking, where rain bearing weather
244 systems are diverted around the immobile blocking high-pressure system (e.g. Figure
245 4). In the southern MDB, atmospheric blocking and the STR that are situated directly
246 over the region are the primary systems responsible for rainfall suppression [*Pook et*
247 *al.*, 2006; *Risbey et al.*, 2008; *Verdon-Kidd and Kiem*, 2009a]. In addition to high-
248 pressure systems that inhibit rainfall, some mechanisms that usually trigger rainfall

(e.g. a cold front) will fail if atmospheric moisture is not available [*Drost and England*, 2008].

Intra-seasonal climate variations across the MDB have been linked to the Madden-Julian Oscillation (MJO), which describes an eastward propagating region of enhanced tropical convection [*Hendon and Liebmann*, 1990]. Typically, the impacts of the MJO on intra-seasonal MDB rainfall vary sub-regionally, seasonally and with the phase of the MJO [*Wheeler et al.*, 2009]. However, across the MDB, the strongest impacts are during the winter and spring months. See *Murphy and Timbal* [2008] and *Wheeler et al.* [2009] for a description of the impacts of the MJO on the southern MDB and regional Australian circulation respectively.

Intra-annual wet and dry periods in the MDB are primarily linked to shifts in the atmospheric circulation inherent to the seasonal cycle. In the northern MDB (at subtropical latitudes), rain bearing systems are more prevalent during the warmer months (approximately November – April), due to the greater influence of tropical weather systems such as those shown in Figure 4a. The opposite is true for the southern MDB, where extra-tropical weather systems dominate (Figure 4b) and rainfall mostly occurs during the cooler months (approximately May – October).

3.2 Inter-annual processes: an update

The El Niño – Southern Oscillation (ENSO) can be responsible for over 20% of local annual rainfall variations in the MDB [*Pittock*, 1975; *McBride and Nicholls*, 1983; *Ropelewski and Halpert*, 1987; *Nicholls*, 1988; *Power et al.*, 1998; *Risbey et al.*, 2009].

271 Seasonally, winter, spring and summer MDB rainfall variations are most
272 strongly associated with ENSO events [*McBride and Nicholls*, 1983; *Risbey et al.*,
273 2009], although the winter relationships may also be due to Indian Ocean influences
274 and their coincidence with ENSO (discussed further below). The effects of ENSO in
275 the MDB also include magnified fluctuations in streamflow volumes compared to
276 rainfall [*Chiew et al.*, 1998; *Wooldridge et al.*, 2001; *Verdon et al.*, 2004b], elevated
277 flood risk during La Niña events [*Kiem et al.*, 2003], and increased risk of drought
278 [*Kiem and Franks*, 2004; *Barros and Bowden*, 2008] and bushfire [*Verdon et al.*,
279 2004a] during El Niño events.

280 The intensity of wet and dry periods in the MDB is not directly proportional to
281 the strength of ENSO events, where the strength of an ENSO event is determined
282 based on the size of the departure from normal sea-surface temperature (SST) or sea-
283 level pressure (SLP) conditions. In fact, the rate at which the state of the Pacific
284 changes from one phase of ENSO to another appears to be just as important as the
285 strength of the ENSO event [*Quinn et al.*, 1978; *Stone and Auliciems*, 1992; *Stone et*
286 *al.*, 1996; *Kiem and Franks*, 2001]. This is demonstrated by the fact that some of the
287 strongest El Niños have not been associated with severe, widespread drought (*e.g.*
288 1997/1998), while other weaker El Niño events have coincided with particularly
289 intense drought (*e.g.* 2002/2003) [*Wang and Hendon*, 2007; *Brown et al.*, 2009]. The
290 non-linear relationship between Australian rainfall variations and the magnitude of
291 ENSO has been attributed to interactions with random atmospheric noise [*Wang and*
292 *Hendon*, 2007], interactions with other climate drivers [*Meyers et al.*, 2007; *Verdon-*
293 *Kidd and Kiem*, 2009a; *Kiem and Verdon-Kidd*, 2010], and the location of the SST
294 anomalies associated with ENSO [*Wang and Hendon*, 2007].

295 *Larkin and Harrison* [2005] and *Wang and Hendon* [2007] showed that
296 Australian rainfall is particularly sensitive to ENSO-like behaviour in the central
297 Pacific. A pattern of central equatorial Pacific sea surface temperature variations has
298 recently been identified by *Ashok et al.* [2007] and defined as an ‘ENSO Modoki’
299 (‘Modoki’ is a Japanese word meaning ‘a similar but different thing’). An El Niño
300 Modoki is characterised by warm central Pacific waters flanked by anomalously cool
301 SSTs to the west and east, separating the Walker Circulation into two distinct
302 circulations. Conversely, a La Niña Modoki is characterised as having cool central
303 Pacific waters that are flanked by warmer than normal SSTs.

304 The location, seasonality and magnitude of the regional Australian climate
305 response induced by an ENSO Modoki event can be stronger than for a traditional
306 ENSO event [*Ashok et al.*, 2009; *Cai and Cowan*, 2009; *Taschetto and England*,
307 2009; *Taschetto et al.*, 2009] and *Cai and Cowan* [2009] also associated La Niña
308 Modoki events with elevated autumn rainfall in the MDB (i.e. a season not typically
309 influenced by traditional ENSO events). However, the work on ENSO Modoki is in
310 its infancy and there have been conflicting conclusions in the literature as to the
311 impacts of El Niño Modoki on the Australian climate. For example, *Taschetto and*
312 *England* [2009] reported strong associations between El Niño Modoki events and
313 reduced rainfall over parts of Australia during autumn, but *Cai and Cowan* [2009]
314 detected no significant correlations during such events. *Lee and McPhaden* [2010]
315 also recently identified a significant increase in the intensity of central Pacific El Niño
316 events since 1982. Given the potential links to the MDB climate, the role of Central
317 Pacific ENSO events must be investigated further.

318 Inter-annual variations in southern MDB winter (JJA) and spring (SON)
319 rainfall have been linked to Indian Ocean SST anomalies [*Nicholls, 1989; Simmonds,*
320 *1990; Drosowsky, 1993; Ashok et al., 2000; Drosowsky and Chambers, 2001;*
321 *Verdon and Franks, 2005*] and the Indian Ocean Dipole (IOD) [*Saji et al., 1999;*
322 *Ashok et al., 2003*]. Verdon and Franks (2005) also showed strong relationships
323 between east Indian Ocean SST anomalies and the northern MDB hydroclimate (in
324 some cases stronger than the Indian Ocean-southern MDB relationships). This is
325 contrary to the commonly accepted understanding that the influence of the Indian
326 Ocean on the northern MDB is weaker than in the southern MDB. Either way the
327 influence of the Indian Ocean on MDB hydroclimate needs further investigation,
328 particularly with respect to the northern MDB.

329 The IOD is characterized by SST anomalies of opposite sign in the east and
330 west of the Indian Ocean Basin, which are coincident with large-scale anomalous
331 circulation patterns. During the phase of the IOD associated with cool east and warm
332 west Indian Ocean SST anomalies, low winter rainfall over the southern MDB is
333 likely, and vice versa for the opposite phase of the IOD [*Saji et al., 1999; Ashok et al.,*
334 *2003; Meyers et al., 2007*]. However, several studies show a similar modulation of
335 rainfall with eastern Indian Ocean SSTs only [*Verdon and Franks, 2005; Cai and*
336 *Cowan, 2008; Nicholls, 2009*], suggesting that the influence of the SST gradient
337 (combined western/central and east Indian Ocean SSTs) on southeast Australian
338 rainfall is perhaps not as important as the state of eastern Indian Ocean SSTs alone
339 [*Nicholls, 1989; Verdon and Franks, 2005*].

340 Several recent studies have also supplied convincing evidence for the non-
341 existence of an equatorial IOD as an independent mode of climate variability and have

argued that it is the result of random variations in the east and west of the Indian Ocean Basin. The two nodes of the IOD are sometimes in phase (i.e. not always negatively correlated), indicating the lack of a consistent dipole structure [Dommenget and Latif, 2001]. Moreover, Dommenget [2007] and Dommenget and Jansen [2009] have shown that the dipole structure can be reconstructed by applying the same statistical technique used to decompose the mode to random noise, suggesting the IOD is simply an artefact of this technique and not a physical structure. Several studies have also suggested that the appearance of an IOD is simply a combination of a byproduct of ENSO and random variations [Nicholls, 1984; Cadet, 1985; Chambers et al., 1999; Allan et al., 2001]. This interaction is discussed further in Section 4.

Along with the weight of evidence suggesting the existence of the IOD as erroneous, its links to Australian rainfall have recently been debated. Ummenhofer et al. [2009a] used a climate model to demonstrate that the eastern pole of the IOD does not regulate Australian precipitation on its own and that a slightly stronger response occurs when there is a forced SST differential between the southern and eastern Indian Ocean. Other studies have shown a stronger response between Australian rainfall and eastern Indian Ocean SSTs [Verdon and Franks, 2005; Cai and Cowan, 2008; Nicholls, 2009] and SSTs to the north of Australia [Smith and Timbal, 2010]. In light of these recent findings it seems that though the Indian Ocean likely has an effect on the MDB climate, the existence of a dipole mechanism as an atmosphere/ocean interaction is questionable. Indeed the strongest evidence suggests southern MDB rainfall variations are more likely associated with SST variability in the eastern Indian Ocean. We stress that, on the balance of current evidence, the Indian Ocean does play a role in regulating the MDB hydroclimate but it is likely that this role is as an intermediary driver only. What is in question is the modulation via an east-west dipole

(i.e. IOD) mechanism and its dependence on or independence of the Indian Ocean teleconnections from ENSO.

Variations in the Southern Annular Mode (SAM) effectively describe variations in the position of the Southern Hemisphere mid-latitude storm track [Karoly, 1990; Thompson and Wallace, 2000; Thompson and Solomon, 2002]. The SAM has links to MDB rainfall that vary regionally and seasonally [Gillett *et al.*, 2006; Hendon *et al.*, 2007; Meneghini *et al.*, 2007]. With a poleward contraction of the mid-latitude storm track, far southern sections of the MDB are more likely to experience lower rainfall during winter [Hendon *et al.*, 2007] due to southward displacement of rain-bearing cold fronts and cyclones. However, during the spring and summer months, anomalously poleward SAM induces changes to the local circulation that draw moist easterly winds inland and increase the likelihood of rainfall across much of the MDB, particularly in the eastern half of the Basin [Meneghini *et al.*, 2007].

The weather systems described in Section 3.1 regulate inter-annual variations in MDB rainfall as their frequency, persistence and intensity changes from year-to-year. For example, the STR changes in average strength and location from year-to-year. A stronger STR has been linked to rainfall suppression in southern Australian rainfall during autumn and early winter, while the position of the STR further north or south than normal is associated with summer rainfall variations [Larsen and Nicholls, 2009].

Atmospheric blocking was also previously described as a regional synoptic process affecting daily rainfall, and its importance as an inter-annual driver of the southern Australia climate has recently been recognised [Risbey *et al.*, 2009]. The

position and intensity of Southern Hemisphere blocking undergoes variations from year-to-year and decade-to-decade [Trenberth and Mo, 1985]. Specifically, the prevalence of blocking systems in key regions has been linked to fluctuations in the frequency of cut-off low pressure systems [Risbey *et al.*, 2008], which are responsible for a significant portion of rainfall in the southern MDB [Pook *et al.*, 2006]. The frequent occurrence of blocking highs centred near 140°E (longitude close to the southwest MDB) favours rainfall in the southern MDB [Risbey *et al.*, 2008; Risbey *et al.*, 2009].

3.3 Inter-decadal processes

In the Pacific Ocean, a coherent pattern of SST and SLP variability operating on multi-decadal timescales has been identified [Zhang *et al.*, 1997]. In the North Pacific, this variability is commonly termed the Pacific Decadal Oscillation (PDO) [Mantua *et al.*, 1997; Mantua and Hare, 2002]. Power *et al.* [1999b] refer to a similar Pacific Basin-wide mode of variability as the Interdecadal Pacific Oscillation (IPO). Importantly, the PDO and IPO time series are highly correlated and represent variable epochs of warming (i.e. positive phase) and cooling (i.e. negative phase) in both hemispheres of the Pacific Ocean [Mantua *et al.*, 1997; Folland *et al.*, 2002; Franks, 2002]. In fact, Folland *et al.* [1999] suggested that the IPO can be regarded as the Pacific wide manifestation of the PDO.

The IPO and PDO have been described as a sustained ENSO-like pattern of Pacific climate variability [Zhang *et al.*, 1997]. However, as noted by Mantua and Hare [2002], two characteristics distinguish the PDO (and IPO) from ENSO: the persistence of PDO/IPO epochs (15-30 years) and the fact that the climatic fingerprint

of the PDO is most dominant in the north Pacific sector with a secondary signature in the tropics (whereas the opposite is true for ENSO).

Links between the IPO/PDO phenomena and climate variability in Australia include decadal and annual-scale fluctuations in rainfall, maximum temperature, water volume transport and wheat crop yield [Power *et al.*, 1999a; Kiem *et al.*, 2003; Kiem and Franks, 2004; Verdon *et al.*, 2004b]. The IPO/PDO primarily influences the eastern Australian climate, which includes the MDB, during the austral spring, summer and autumn by inducing variations in the South Pacific Convergence Zone, which tends to be active during these months [Folland *et al.*, 2002].

The IPO/PDO regulates the eastern Australian climate indirectly by modulating both the magnitude and frequency of ENSO impacts [Power *et al.*, 1999b; Kiem *et al.*, 2003; Verdon *et al.*, 2004b; Cai and Cowan, 2009]. When the IPO/PDO is in a warm phase, the relationship between ENSO and Australian rainfall is weakened, while it is strengthened during the cool phase [Power *et al.*, 1999a]. The greatest effect of this modulation is a magnified response of rainfall and streamflow to La Niña events during a cool IPO/PDO phase. During the cool (i.e. negative) IPO/PDO phase, wet events are likely to be wetter and more frequent than during a neutral or warm IPO/PDO phase, elevating flood risk in the MDB [Kiem *et al.*, 2003; Verdon *et al.*, 2004b]. Conversely, during the warm (i.e. positive) IPO/PDO phase wet events are less frequent and not as wet as they are during the IPO/PDO cool phase which results in an increased risk of drought across the MDB and other parts of eastern Australian [Kiem and Franks, 2004; Verdon-Kidd and Kiem, 2009a]. Verdon and Franks [2006] confirmed that the relationships between IPO/PDO phase and the frequency of ENSO events is consistent over the past 450 years by examining

paleoclimate reconstructions of the two climate modes. While Lough [2007] showed that the relationship between ENSO, IPO and rainfall/streamflow in northeast Queensland is consistent for at least the last 400 years.

Also important to note is the strong and statistically significant relationships between decadal rainfall in the MDB and SSTs in the Tasman Sea north of New Zealand and south of 15°S – wetter decades are associated with warmer SSTs in the Tasman Sea [Power *et al.*, 1999a]. This Tasman SST-MDB rainfall relationship is also evident on inter-annual time scales. The effect of this association on regional circulation patterns is not yet understood. However, it is reasonable to suppose that larger rainfall totals would be caused by warmer, moist air being transported to, and converging over, the Australian mainland [White *et al.*, 2003].

Decadal and multi-decadal scale variations in SSTs and surface pressures around Australia that are reminiscent of an ENSO pattern have been linked to multi-year summer-time droughts in eastern Australia [White *et al.*, 2003; White *et al.*, 2004]. Such droughts may be due to random fluctuations of ENSO [Kestin *et al.*, 1998] or they may be due to some other as yet unknown process(es). The established statistical relationships suggest a connection between decadal-scale SST variability and fluctuations in MDB rainfall. However, the physical mechanisms which cause the decadal-scale SST variability and the links between changes in SST and regional-scale variability in synoptic patterns (and rainfall) are currently unknown and require further investigation.

In addition to the natural variability described above, anthropogenic influences will very likely also be responsible for future multi-decadal scale climate variations in the MDB [CSIRO and BoM, 2007; IPCC, 2007]. Anthropogenically-induced changes

in some aspects of the regional Australian climate have already been detected [Karoly and Braganza, 2005]. There are a wide range of projected impacts for the MDB climate (i.e. ‘wetter and warmer’ or ‘drier and warmer’) and unfortunately, there is no clear signal in the direction of these changes across the MDB.

The uncertainties primarily stem from large differences between future rainfall changes in the MDB projected by global climate models in response to future greenhouse gas emission scenarios. While these projections consistently show increasing temperatures across the MDB over the 21st century, they do not show consistent changes in rainfall [Sun *et al.*, 2011]. One regional exception is the southern MDB, for which many climate models consistently project drying. However, the magnitude of this drying varies considerably between models [Chiew *et al.*, 2008] and the dynamical mechanisms behind this drying have not yet been identified. Given the potential for anthropogenic warming to be associated with significant negative impacts across the MDB [Alexander and Arblaster, 2009; BoM, 2010], the uncertainty associated with climate model projections must be addressed so that the contribution of anthropogenic forcing to inter-annual, multi-decadal and longer changes in MDB can be properly assessed. This numerous sources of uncertainty associated with global climate model projections for the MDB are discussed further in Section 5.

4. Interactions between hydroclimatic processes: a missing link in our understanding?

4.1 Interactions between climate processes

As single processes alone account for less than 20% of monthly rainfall variability [Risbey *et al.*, 2009], it is unlikely that the climate drivers influential on the MDB are independent of each other or act to drive the MDB climate in isolation [Risbey *et al.*, 2008; Verdon-Kidd and Kiem, 2009b; Kiem and Verdon-Kidd, 2010]. Deducing the interactions between climate drivers and their subsequent impact on the Australian hydroclimate is only an emerging area of research, but one that is crucial to better capturing the causes of variations in the MDB climate.

There is increasing evidence that the mean state of the atmosphere/ocean system, which is partially modulated by the inter-annual and inter-decadal processes previously described, plays a part in regulating the occurrence of daily weather events. For example, the large-scale climate processes described in Section 3 have been linked to variations in the positions of the jet streams, regulation of moisture availability and other aspects of the atmosphere/ocean system, as well as variations in weather systems [Risbey *et al.*, 2008; Verdon-Kidd and Kiem, 2009a].

The characteristics of weather systems, including their location, frequency of occurrence and intensity, show dependence on intra-seasonal, inter-annual and decadal drivers of climate such as the MJO, ENSO and the IPO/PDO [Nicholls and Kariko, 1993; Pezza *et al.*, 2008]. The intensity of cyclones and anticyclones in the mid-latitudes increases and their frequency decreases when there is a strong warm phase of the PDO [Pezza *et al.*, 2007]. Verdon-Kidd and Kiem [2009a] also found that warm phases of the IPO decrease the likelihood of wet weather events in parts of the MDB, while cool phases increase this likelihood, and vice versa for dry weather events.

507 Variations in the prevalence of atmospheric blocking have been linked to the
508 state of ENSO, with blocking frequency and associated rainfall becoming more
509 prominent during La Niñas and less prominent during El Niños [*Risbey et al.*, 2008].
510 Weather features such as pre-frontal troughs and ‘easterly-dip’-type patterns are more
511 prominent during La Niñas, and broad high pressure systems across southeastern
512 Australia and a northward retraction and weakening of easterly troughs are more
513 prominent during El Niños [*Verdon-Kidd and Kiem*, 2009a]. The wetter and drier
514 phases of SAM and Indian Ocean SSTs are similarly linked to weather systems that
515 are more or less likely to enhance or suppress rainfall in the MDB [*Hendon et al.*,
516 2007; *Verdon-Kidd and Kiem*, 2009a; *Kiem and Verdon-Kidd*, 2010].

517 We present analysis in Figure 5 demonstrating the connections between
518 climate processes operating on inter-annual and daily time scales. *Pook et al.* [2006]
519 found that at least 80% of April–October heavy rain days (defined as days with
520 accumulations above 25 mm) were associated with cut-off low-pressure systems in a
521 domain covering the far southwest MDB. They also showed that cut-off low-pressure
522 systems strongly modulate inter-annual rainfall there. Given that Section 3.2 outlined
523 the modulation of inter-annual rainfall in the MDB by ENSO, SAM and the Indian
524 Ocean, a logical hypothesis is that these remote drivers partially act by modulating the
525 number of cut-off low-pressure systems that influence the region. This influence was
526 examined here by using heavy rain days as a proxy for cut-off lows.

527 The number of heavy rain days was calculated at seven stations for every
528 April–October period from 1970–2002, the same period used by *Pook et al.* [2006] for
529 their analysis. All stations fall within the *Pook et al.* [2006] domain and come from
530 the *Lavery et al.* [1992] high-quality daily rainfall network. The average number of

heavy rain days during years in a particular extreme state of the SAM, ENSO and eastern Indian Ocean SSTs were compared to neutral years for each index. The SAM, ENSO and eastern Indian Ocean SSTs were represented by the SAM index of *Marshall* [2003], the Southern Oscillation Index (SOI) of *Troup* [1965] and the eastern pole of the Dipole Mode Index (DMIeast) of *Saji et al.* [1999], generated from the global HadISST sea-surface temperature data set [*Rayner et al.*, 2003]. A positive (negative) phase of each driver was defined if the standardized index was above (below) 0.5 (-0.5) standard deviations, giving about 30% of years in each of the positive or negative phases. All indices were standardized over the 1970–2002 period. To determine if the mean frequency of heavy rain days during a particular phase of a driver was statistically significantly different from neutral years, a 95% confidence interval was generated from neutral years. The mean number of rain days from 1000 bootstrap replicates of n neutral years were used, where n was the number of years when the inter-annual driver was in its positive or negative phase.

Every station in the domain had a statistically significant link between April–September heavy rain days and ENSO, with a higher than average number of heavy rainfall days during La Niña years and a lower than average number during El Niño years (Figure 5). This result was the same whether SOI or SSTs from the Nino3.4 region were used to represent ENSO and is consistent with the links described between ENSO and cut-off lows in the region by *Pook et al.* [2006]. All but one station had a lower than average number of heavy rain days during negative SAM events, with three stations showing a statistically significant difference. These results may reflect the influence of the SAM during the austral spring, where negative SAM is associated with decreased rainfall in the region [*Hendon et al.*, 2007]. The majority of stations also had significantly more heavy rain events during years with warmer

than normal eastern Indian Ocean SSTs and fewer heavy rain events when these SSTs were cooler than normal. The results here suggest that all three major drivers of interannual climate variations in the region partially regulate rainfall by changing the frequency of heavy daily rainfall events, which in turn are likely to be via modulation of the frequency of cut-off low pressure systems.

The above analysis showed that large-scale climate drivers play a role in regulating daily weather events. However, the large-scale drivers themselves also undergo decadal and multi-decadal scale variations. These variations may be largely independent or they may co-occur, indicating relationships between processes that, in turn, affect regional climates.

Figure 6 shows fluctuations in the relationships between indices representing ENSO, SAM, Indian Ocean SST variability and STR location and intensity for running 30-year periods from 1905–2004. The indices were chosen so the longest period possible could be analysed. The SOI represents ENSO variations and an extended reconstruction of the Marshall [2003] SAM index by *Jones et al.* [2009b] was used as the Marshall [2003] index is available from 1958 only. The eastern pole of the DMI [*Saji et al.*, 1999] represents eastern Indian Ocean SSTs. Despite the fact that we are reluctant to accept the IOD as a physical atmosphere/ocean processes for the reasons outlined in Section 3, we also include the DMI (representing the IOD) in our analysis for a later discussion surrounding evidence that any large-scale climate variations in the Indian Ocean may be partially linked to ENSO. The latitude and intensity of the STR [*Drosowsky*, 2005] is also assessed as an inter-annual driver of MDB rainfall variations. All indices were detrended by removing the line-of-best-fit

over the 1905–2004 period, computed using linear regression, to highlight relationships on inter-annual time scales only.

The fluctuations in the relationships between inter-annual drivers of the MDB climate vary between pairs of drivers and season. For example, summer (December–February) STR intensity has a statistically significant relationship with SAM that has remained fairly consistent from 1905–2004. Conversely, the relationship between the inter-annual variations in ENSO and the eastern Indian Ocean SSTs were barely statistically significant in the 1930s (correlations around -0.35), while the 30 years centred on 1970 had a correlation of almost -0.9. These indicate large changes in the relationship between ENSO and the eastern Indian Ocean during the 20th Century. There are consistent statistically significant relationships between SAM and STR intensity from winter through to summer (June–February) and between SAM and STR latitude during winter and spring (June–November), perhaps highlighting broader scale fluctuations in the Hadley circulation. Interestingly, there has been a consistent strengthening of the relationship between the SAM and STR latitude during the austral autumn (March–May) where correlations in the early 1900s were insignificant and negative and were statistically significant and positive from around 1960 (Figure 6). As the indices were detrended prior to computation of the correlations, the strengthening of this relationship over time is probably not associated with the trends that have occurred in both processes since around this time [Marshall, 2003; Larsen and Nicholls, 2009]. The trend may reflect poor data coverage for calculation of the SAM prior to the 1960s. However, if this were the case, a step-function, rather than a monotonic trend might be expected.

Previous authors have shown how interactions between various large-scale climate drivers impact on the MDB climate [Risbey *et al.*, 2009; Silvestri and Vera, 2009; Verdon-Kidd and Kiem, 2009a]. We have also previously argued that the IOD is not a physical atmosphere/ocean interaction (Section 3) with many studies providing evidence that it is a combination of a byproduct of ENSO and stochastic variations [Nicholls, 1984; Cadet, 1985; Chambers *et al.*, 1999; Allan *et al.*, 2001]. The extreme phases of ENSO and IOD are also often ‘phase locked’ meaning that there is a high probability that a La Niña will occur with warm, and an El Niño with cool, eastern Indian Ocean SSTs [Meyers *et al.*, 2007]. As these coinciding phases are indicative of wet or dry conditions for both ENSO and the IOD, the result is often an amplification of the rainfall signature [Meyers *et al.*, 2007]. The synchronicity between extreme ENSO and IOD variations suggests dependence between the two and Allan *et al.* [2001] reported significant lag correlations in ENSO and IOD indices.

Using the IOD and ENSO indices previously described from 1905–2004, we found statistically significant correlations of -0.57 between spring indices, and -0.59 when a lag correlation was calculated between the winter (June–August) SOI and the DMI in the subsequent spring (September–November). Both correlations are strongly indicative of dependence between the two during the time when the Indian Ocean has its greatest influence on MDB rainfall. Furthermore, temporal variations in correlations between September–November SOI and DMI for running 30-year periods from 1905–2004 show consistent statistical significance from at least 1960, when data is most reliable (Figure 6). Moreover, when the SOI was correlated against the eastern pole of the DMI only (i.e. eastern Indian Ocean SSTs) there were statistically significant relationships during winter, spring and summer.

626 However, others have presented evidence that Indian Ocean SST anomalies
627 can occur irrespective of the state of the tropical Pacific Ocean [*Nicholls*, 1989; *Saji et*
628 *al.*, 1999; *Webster et al.*, 1999]. *Saji et al.* [1999] report that the IOD is the most
629 active during the austral winter (JJA) and that there is a lack of statistically significant
630 correlations between winter IOD and ENSO indices, potentially indicating
631 independence. *Webster et al.* [1999] demonstrated that the Indian Ocean can exhibit
632 strong ocean-atmosphere-land interactions that are self-maintaining and capable of
633 producing large perturbations that are independent of ENSO. *Fischer et al.* [2005]
634 used a GCM to study the triggers of the IOD and showed that two types of IOD may
635 actually exist, one entirely independent of ENSO and the other a consequence of
636 tropical Pacific conditions (i.e. ENSO). This is supported by the fact that the IOD is
637 not always phase locked with ENSO and that there are few incidences where a La
638 Niña coincides with a positive IOD and vice versa (i.e. few incidences where El Niño
639 coincides with negative IOD). Regardless, none of these studies provide a physical
640 mechanism for the IOD as a climate process that is independent of ENSO. As such,
641 we continue to argue for the non-existence for an IOD and like previous studies,
642 suggest that any apparent ‘IOD’ is probably the result of combined ENSO influences
643 and stochastic variations, or random variations alone. However, given the conflictions
644 in the literature, more work needs to be undertaken to establish if this is the case. As
645 mentioned previously (Section 3.2) this is not to say that the Indian Ocean is not an
646 important influence on MDB hydroclimate but that the influence is more likely to be
647 driven by eastern Indian Ocean SSTs rather than the east-west dipole (i.e. IOD). This
648 is demonstrated by Verdon and Franks (2005) who found that the relationship
649 between eastern Indian Ocean SSTs and eastern Australian hydroclimate still holds
650 when ENSO events are removed.

The interaction between SAM and ENSO and their combined impact on Australian rainfall has received little attention in the literature. From correlation analysis performed here, the relationship between SAM and ENSO is not significant during any season, except perhaps in more recent years during the austral autumn (Figure 6). Correlations between ENSO and SAM using data from 1905–2004 at lags of one to three months were generally not statistically significant. Again, a potential exception is during the austral autumn (March–May) when the correlation between SAM and ENSO lagged by one and two months was marginally significant at the 95% level ($r = 0.21$ and $r = 0.22$ respectively, $n = 100$). However, neither driver shows a statistically significant relationship with rainfall in the MDB during this season [Hendon *et al.*, 2007; Meneghini *et al.*, 2007; Risbey *et al.*, 2009]. In general, the evidence presented here suggests that SAM and ENSO are largely independent modes of variability. However, Karoly [1989] described covariations between the Southern Hemisphere middle latitude circulation and ENSO events, which perhaps indicates a relationship between SAM and ENSO in summer.

Despite the fact that ENSO and SAM appear to act in an independent manner, there are competing effects between the two that influence MDB seasonal rainfall. Kiem and Verdon-Kidd [2009; 2010] reported that dry conditions during autumn are more likely if an El Niño event occurs in combination with a positive SAM. Previous La Niña events have not necessarily been associated with above-average rainfall in the southern MDB [Gallant and Karoly, 2009], which may be due to interactions with coinciding SAM events that place the storm track further south than normal [Kiem and Verdon-Kidd, 2009; 2010].

An example of the impacts of competing SAM and ENSO phases on MDB rainfall are illustrated in Figure 7. The rainfall anomalies were generated using the operational Australian Bureau of Meteorology AWAP rainfall grids [Jones *et al.*, 2009a] from 1905–2004. The Jones *et al.* [2009b] SAM index, described previously as an extension of the Marshall [2003] index, was used to maximise the number of years available for analysis. As previously, the SOI represents ENSO variability. A positive SAM or ENSO event was defined when the standardized indices (relative to the 1905–2004 period) exceeded 0.5 standard deviations. However, the results were similar when thresholds of between 0.5 and 1 standard deviation were applied and when SSTs from the Niño3.4 region were used to represent ENSO.

In all seasons, when combinations of the extreme phases of each driver co-occurred the SAM typically enhanced or tempered the impact of ENSO, depending on the phase of the SAM. However, the extent of this influence depended on the season. Specifically, the strength of the relationship between MDB rainfall and each process tended to dictate the influence each had on seasonal rainfall. For example, neither the SAM nor ENSO, when considered in isolation, have a strong relationship with autumn (March–May) rainfall in the MDB but when SAM-ENSO interactions are analysed some autumn rainfall variability is explained (e.g. Kiem and Verdon-Kidd, 2009, 2010]. In comparison, winter (June–August) rainfall has a stronger relationship with both SAM and ENSO [Risbey *et al.*, 2009], making competing influences more noticeable (Figure 7). During the austral winter the southern MDB was typically drier, while the northern MDB was wetter, for a co-occurring La Niña and positive SAM event, compared to a La Niña event occurring in isolation. Conversely, the drier conditions in the southern MDB during past El Niño events have been enhanced by positive SAM and tempered by negative SAM.

Note that the frequencies at which combined events occurred were small in several cases. So, producing composites from n randomised years tested the statistical significance, where n was equal to the number of years used to produce each composite (see Figure 7). Statistical significance was defined if the value of the composite being tested was larger/smaller than 97.5% of the randomised composites.

During combined positive SAM and El Niño, and negative SAM and La Niña, the rainfall anomalies in Figure 7 were statistically significant across most of the MDB (not shown). Interestingly, during JJA, the extreme phases of ENSO during neutral SAM had few statistically significant rainfall anomalies in the southern MDB. Thus, across the MDB, particularly the southern half, there is significantly enhanced drying and wetting respectively when positive SAM/El Niño or negative SAM/La Niña phases co-occur.

For combined positive SAM/La Niña events, the rainfall anomalies were not statistically significantly different in the southern MDB. However, when La Niña combined with negative or neutral SAM conditions it was statistically significantly wetter in this region, indicating that positive SAM may have some tempering effect. Similarly, for combined negative SAM/El Niño years, significant drying was limited to the far northeast of the Basin. However, for neutral SAM/El Niño, significant drying extended across the northern and eastern two-thirds of the Basin and across most of the MDB for a positive SAM/El Niño combination.

Interactions between climate processes have also been demonstrated between drivers operating on decadal and inter-annual time scales. The IPO/PDO regulates the eastern Australian climate indirectly by modulating both the magnitude and frequency of ENSO impacts [*Power et al.*, 1999b; *Kiem et al.*, 2003; *Verdon et al.*, 2004b; *Cai*

and Cowan, 2009]. When the IPO/PDO is in a warm phase, the relationship between ENSO and Australian rainfall is weakened, while it is strengthened during the cool phase [Power *et al.*, 1999a]. The greatest effect of this modulation is a magnified response of rainfall and streamflow to La Niña events during a cool IPO/PDO phase. During the cool (i.e. negative) IPO/PDO phase, wet events are likely to be wetter and more frequent than during a neutral or warm IPO/PDO phase, elevating flood risk in the MDB [Kiem *et al.*, 2003; Verdon *et al.*, 2004b]. Conversely, during the warm (i.e. positive) IPO/PDO phase wet events are less frequent and not as wet as they are during the IPO/PDO cool phase which results in an increased risk of drought across the MDB and other parts of eastern Australian [Kiem and Franks, 2004; Verdon-Kidd and Kiem, 2009a].

Given the temporal fluctuations in the relationships between the major climate drivers, further work is needed to understand the mechanisms that cause these fluctuations and how they impact on regional climates, such as the MDB. The long-term variations could stem from random variations [Kestin *et al.*, 1998], interactions with unknown climate processes on numerous time scales [Power *et al.*, 1999a], other external forcings [Meehl *et al.*, 2006], or a combination of all or some of these. Also unclear at this stage is how large-scale climate processes such as ENSO, Indian Ocean SSTs, SAM, STR and IPO/PDO might be affected by anthropogenic climate change.

4.2 Hydrological drivers and their interactions with climate processes

Interactions influencing the MDB hydroclimate (e.g. rainfall, temperature, runoff, streamflow etc.) are not limited to those between climate processes. Hydrological and land surface processes also play an important role in regulating hydroclimatic variability in the MDB. Rainfall and surface temperature persistence

are related to soil moisture, which can retain some memory of the recent climate [Timbal *et al.*, 2002]. Antecedent land surface conditions play an important role in runoff and streamflow variability [Chiew *et al.*, 1998; Kiem and Verdon-Kidd, 2009]. CSIRO [2008] also suggests that it is likely that after a prolonged dry period, there is less connectivity between the subsurface storage and the river system, and therefore significant amounts of rainfall and recharge are required to fill the subsurface storage before runoff can occur.

It is likely that vegetation feedbacks also play a role in regulating regional climate and that extensive land clearance across the Australian continent has contributed to some long-term climatic trends [Murphy and Timbal, 2008]. Rainfall recycling feedbacks (and the memory the system has of previous rainfall) is poorly understood because the soil moisture-vegetation-rainfall feedbacks are complex. However, it is believed to be important in determining downwind rainfall in continental areas [Koster *et al.*, 2004]. This is an area of ongoing research that also has, as an added complexity, the difficulties and computational limitations associated with integrating land surface models with climate models.

5. A framework for focussing climate information for natural resource management

Knowledge of the MDB hydroclimate, and its driving mechanisms, assists NRM in developing appropriate management strategies. As this environment changes management strategies must be adapted. Given that the MDB has large natural climate cycles, and more recently the possibility of anthropogenic influences, it is critical that

770 NRM is better able to isolate the potential causes of extremes or changes in the
771 climate.

772 There are numerous, complex processes modulating the MDB hydroclimate
773 (see Sections 3 and 4) and sifting through this vast amount of knowledge can be an
774 arduous task. So, we present a broad framework that summarizes the relevant climatic
775 information and assists in isolating the possible causes of a climatic event. It is
776 important to note that this is a simplified framework for a complex problem and will
777 not provide definitive answers. This is because the processes previously presented do
778 not equal the sum of knowledge required for complete understanding of a climate
779 system that is substantially chaotic and involves complex non-linear and non-
780 stationary interactions – as well as several significant knowledge gaps. However, the
781 framework does allow the user to qualitatively estimate the likelihood of a cause of a
782 climatic event. We stress that this framework is not intended to be a decision-making
783 tool – only to better focus understanding.

784 The framework breaks down a climatic event into its fundamental
785 components, isolating i) spatial signatures, ii) temporal signatures and iii) small-scale
786 evolution. Spatial information identifies the regional coverage of the event, including
787 where it occurred and over what size area. Temporal signals identify the persistence
788 of the event, including any seasonality or recurrence. For example, a single season
789 might experience an extreme climatic event but this may reoccur for multiple years.
790 Small-scale evolution deconstructs the event to isolate the small-scale features. For
791 example, the make-up of the daily rainfall distribution causing a seasonal anomaly –
792 is the deficit due to a lack of rain days, or a decrease in rainfall intensity or

magnitudes? Small-scale evolution also includes assessing changes in weather systems.

Following the characterisation of an event using the above framework, the event's features can be compared to those typical of the known climatic drivers described in Sections 3 and 4. This comparison allows the user to rank the possible mechanisms, where the ranks are based on the consistency between a feature and the known impacts of a climatic process. Allowances must be made where the consistency between the fundamental elements of the event and the climatic driver are unknown or the uncertainty is large. The consideration that there are likely to be processes (or interactions and feedbacks) of which we are currently unaware that are affecting the event must also be made. These caveats are discussed in the case study presented below.

5.1 Case study: identifying potential causes of the Big Dry (c. 1997–2010)

The framework presented above is now applied to a case study, namely, the Big Dry (c. 1997–2010). Here, we focus solely on the rainfall deficits to simplify the framework for presentation. However, formal event attribution for NRM should be applied to multiple variables (i.e. incorporate knowledge of other changes such as soil moisture, temperatures etc.). The major characterising features of the Big Dry are identified below and each feature is tagged 1–7 for later comparison with climate processes.

1. Spatial signatures

The rainfall deficits were mainly confined to the southern MDB¹. The largest deficits were in the far southeast and southwest of the region (Figure 3). Note that drought was also experienced in the northern MDB from 1997-2006, however, for this

exercise the northern MDB drought is considered to be a different event to the Big Dry, which is characterised by rainfall deficits in the southern MDB from 1997-2010.

2. Temporal signatures

The 13-year rainfall deficit was primarily driven by consistently lower than normal rainfall during autumn². However, several individual years also experienced deficits during winter and spring³ [Verdon-Kidd and Kiem, 2009b]. While deficits generally did not last more than a few consecutive seasons, there was a distinct lack of periods with very high rainfall⁴ [Gallant and Karoly, 2010].

3. Small-scale evolution

There was a lack of high one-day rainfall totals⁴ [Murphy and Timbal, 2008; Verdon-Kidd and Kiem, 2009b], which is consistent with a reduction in the amount of rainfall associated with cut-off low pressure systems over this period⁵ [Pook *et al.*, 2006; McIntosh *et al.*, 2007] and an absence of persistent pre-frontal troughs that aid the penetration of rain producing cold fronts into the southern MDB⁶ [Verdon-Kidd and Kiem, 2009a; Alexander *et al.*, 2010]. The recent drying has also coincided with an increase in regional surface pressure⁷ [Drosowsky, 2005; Timbal and Murphy, 2007; Larsen and Nicholls, 2009; Williams and Stone, 2009; Alexander *et al.*, 2010]. The Big Dry has also been associated with abnormally high temperatures [Nicholls, 2004; Gallant and Karoly, 2009]. However, the causal mechanisms behind the relationship between elevated temperatures and the hydroclimate (e.g. evaporation and streamflow) are largely unknown when compared with changes in other atmospheric conditions such as radiation, humidity and wind [Donohue *et al.*, 2010]. This is another area in need of further study.

840 As the drought primarily occurred on inter-annual and longer time scales with
841 symptomatic small-scale changes (i.e. weather systems), Table 1 present simplified
842 summaries of climate processes (from Section 3) relevant to these time scales. Table 2
843 then compares the seven main features of the Big Dry to this information, thus
844 focusing causal candidates. Note that while the simplified comparison in Table 2
845 identifies where links between drought features and climate processes are unknown, it
846 does not incorporate the uncertainties described in Sections 3 and 4, which are very
847 important (see later discussion). Further, longer term trends in some inter-annual
848 processes have recently been identified including an increase in the intensity of the
849 STR [*Drosowsky, 2005; Timbal and Murphy, 2007; Larsen and Nicholls, 2009;*
850 *Williams and Stone, 2009*] and a poleward retraction of the mid-latitude storm belt
851 [*Frederiksen et al., 2011*] which is consistent with trends towards a more positive
852 SAM [*Marshall, 2003*]. As such, these trends have also been included and assessed in
853 Table 2 as potential causal mechanisms of the Big Dry.

854 Based on the number of consistencies, unknowns and inconsistencies between
855 each drought feature and climate process indicated in Table 2 it is then possible to
856 rank the most likely causal mechanism(s) of the Big Dry with the highest ranks given
857 to those processes with the most consistencies and least inconsistencies. Note this
858 method is biased towards those processes that are most well understood and as such
859 processes that included many unknowns should not necessarily be ruled out as
860 possible causes.

861 Using the above approach the most likely causal mechanisms behind the Big
862 Dry were (in order); a southerly shift in the storm track; ENSO/SAM interactions,
863 increases in STR intensity; anthropogenic climate change; more positive SAM; and

the IPO/PDO. Less likely was Indian Ocean variability and ENSO, when considered as isolated processes, mainly due to the inconsistencies in the seasonality of the most persistent rainfall deficits. While it is likely that these processes contributed to a worsening of the drought, on their own they were probably not responsible for the majority of the rainfall deficits [Verdon-Kidd and Kiem, 2009b]. Also worth noting, though there is no evidence of this in existing literature, is the possibility that the Big Dry was caused by interactions between IPO, ENSO and SAM. This inference is based on the following reasoning: IPO modulates the magnitude and frequency of ENSO impacts, the impacts of ENSO are also modulated by SAM and vice versa, therefore it is possible that IPO also influences SAM impacts (either directly or via IPOs modulation of ENSO impacts). This hypothesis is currently under investigation.

The high ranking of ENSO/SAM interactions supports the point made previously (see Section 4, Figure 5, Figure 6, Figure 7), that all climate processes have some degree of interaction and should not be taken as isolated causes. For example, the three La Niña events occurring during the Big Dry were been associated with unusually low rainfall in the context of historical events [Gallant and Karoly, 2009]. Kiem and Verdon-Kidd [2009] attribute this to a compounding influence from a positive SAM and this is consistent with Figure 7. The lack of La Niña events during the 1990s (i.e. the initiation of Big Dry) is also consistent with the IPO being in a positive phase [Kiem *et al.*, 2003].

The rankings from Table 2 are also in agreement with Nicholls [2009] and Verdon-Kidd and Kiem [2009b] who suggested that a consistently positive SAM since the 1990s, associated with a poleward retraction of the mid-latitude storm track [Frederiksen *et al.*, 2011], may be responsible for the recent trends in southeast

Australian rainfall. However, there are some conflicts between these results and other studies that show there are no significant associations between southeast Australian autumn rainfall and the SAM [Hendon *et al.*, 2007; Timbal and Murphy, 2007; Risbey *et al.*, 2009]. However, the critical difference is that the studies finding no significant associations have only examined the SAM in isolation as opposed to considering interactions with other processes (e.g. Figures 6 and 7), which potentially enhance/suppress typical impacts [Kiem and Verdon-Kidd, 2010].

The association between the intensity of the STR and rainfall variations has also previously been suggested as a potential cause [Timbal and Murphy, 2007; Timbal *et al.*, 2007; Murphy and Timbal, 2008; Larsen and Nicholls, 2009]. Though plausible, it is unclear whether an increase in STR intensity is the ultimate cause. Indeed, Figure 6 shows positive relationships between STR intensity and SAM during autumn and winter that indicate that the SAM is associated with up to 44% of the variance in STR intensity (the largest rainfall declines have been reported during late autumn and early winter [Murphy and Timbal, 2008; Verdon-Kidd and Kiem, 2009b]).

All hypotheses of the cause of the Big Dry have a common similarity. That is, all involve decadal scale variations in the major climate drivers and how they influence southern MDB rainfall, and that the causes are possibly linked, either via interactions with each other or via some ultimate cause, which may include anthropogenic climate change [Thompson and Solomon, 2002; Arblaster and Meehl, 2006]. Indeed, the possible climate processes responsible for the drought identified in Table 2 are probably a combination of both natural and anthropogenic sources. However, although anthropogenic climate change was identified as a possible or

partial cause of the drought there are very large uncertainties stemming from many sources that surround this statement.

The most obvious source of uncertainty is that there are numerous aspects of the climate system that are still not well understood and probably many more that are yet to be identified. This is particularly true of decadal and longer-scale processes for which knowledge is fundamentally limited by a lack of observations (e.g. the MDB only has 110 years, or 11 independent decades, of climate records). This makes it particularly difficult to gauge the true extent of decadal-scale variations in MDB hydroclimate (i.e. to put the Big Dry into context) and to differentiate between the impacts of natural inter-decadal to centennial variability and anthropogenic climate change. This can be overcome by continuing two major research streams.

The first involves complementing the limited instrumental record (approximately 100 years) by extending the historical record using various sources of palaeoclimate information [Verdon and Franks, 2006; Lough, 2007; Gallant and Gergis, 2011]. Verdon and Franks [2006] estimated variations in east Australian rainfall using reconstructions of the PDO for the past 400 years. More recently, Gallant and Gergis [2011] and Gergis *et al.* [2011] developed an experimental reconstruction of River Murray streamflow and southeast Australian rainfall respectively, and showed that the streamflow deficits associated with the Big Dry were very rare, but not necessarily unprecedented, during the period 1783–1988. In both studies, palaeo records indicate there have been large decadal-scale variations in the east Australian hydroclimate prior to the instrumental record. Palaeoclimate reconstructions are useful for estimating the bounds of past climate variability. However, interpreting the physical processes behind the pre-instrumental variations is

935 difficult. This is something that can only be properly studied via complementary
936 modelling studies.

937 To date, much of our understanding of the processes driving the MDB climate
938 has been established through the identification of consistent patterns and modes of
939 variation in the atmosphere/ocean system. As such, the second approach to
940 understanding decadal-scale hydroclimate variations, which as mentioned is difficult
941 with limited instrumental data, is via studies utilising climate models that represent
942 the fundamental physics of the atmosphere/ocean system. However, this presents a
943 further problem, as climate models can still not sufficiently model all these processes
944 that are known to drive regional hydroclimatic variability. A subsequent issue is that
945 their teleconnections with regional climates are not well captured. Thus, while climate
946 models may suggest a particular future change that is consistent with a present-day
947 trend, it is difficult to ascertain whether the mechanisms behind these trends in model-
948 space are consistent with reality. This is a knowledge gap that requires immediate
949 attention.

950 Given the lack of understanding about the physics behind both anthropogenic
951 and natural processes, we suggest that if a framework similar to that presented here is
952 utilised by NRM, that a weighting should be applied to each process that is inversely
953 proportional to the uncertainty (i.e. the higher the uncertainty the less weight given to
954 that causal process). This weighting factor may be arbitrary or based on some
955 quantitative measure of uncertainty associated with each process. Developing such
956 weighting factors is a complex process and is outside the scope of this paper. So at
957 present, the best we can do given the current state of knowledge is to propose how the
958 processes we understand, and the interplay between them, fit in the context of this

event (Table 2). However, it is important to remember that the certainty of our attribution is proportional to our understanding and hence, is limited by it.

6. Concluding remarks

This paper demonstrates advances in our understanding of the climate processes influencing the MDB, however, it also highlights that there is much that is not well understood. The framework presented in Section 5 is designed to improve understanding to better focus NRM. So, in conclusion we summarise the key areas of research that we believe will assist in improving the reliability of hydroclimatic insights and forecasts for the MDB (on seasonal to decadal scales) and better quantification of climate related risk for NRM.

i) Expanding data records – instrumental and palaeoclimate-proxies

A maximum of 60 to 110 years of instrumental data are available in the MDB and other regions that regulate its climate (e.g. the Southern Ocean). As such, reliable estimates of climate variations on multi-decadal and longer time scales are not possible due to limited degrees of freedom. This is a problem for water management, which often assumes that the instrumental hydroclimate records are representative of current and future climatic conditions. Given the lack of long- term instrumental data, research investment into expansion of the instrumental record and the use of palaeo records is recommended.

ii) Improving understanding of interactions between climate drivers

In Section 4.1, we performed some simple analysis to highlight interactions between the processes driving the MDB climate on multiple time-scales. From this analysis, it is clear that a better understanding of climate driver interactions on all time

scales is required. Until such knowledge is gained it is difficult to: i) know how to assess their impacts relative to one another; ii) determine the extent of their independence and how their contributions vary spatially and temporally; iii) discriminate between impacts associated with natural and anthropogenic climate variations; iv) develop (and/or improve) climate models to have greater confidence in future climate projections – it is unclear how climate models (either statistical or dynamical) can simulate climate process that we do not yet properly understand.

iii) Improving understanding of interactions between climatic and hydrological processes

Section 4.2 described the limited body of work examining interactions between ocean-atmosphere circulation patterns and hydrological/land-surface processes. Given its potential importance, further examination of i) connections between antecedent hydrological conditions and/or land cover change and regional climates; ii) the mechanisms driving the apparent relationship between increased temperature and decreased streamflow; iii) the possibility of a rainfall recycling phenomena [Koster *et al.*, 2004] in the MDB, is required.

iv) Improving the representation of climate processes in climate models

Climate models provide a complementary way of examining variations in MDB hydroclimate. However, improving how climate models simulate the processes that drive the MDB hydroclimatic variability is crucial, as is the need for regionally specific information. Improved modelling capabilities will assist with the previous three research aims and vice-versa.

1004 The research areas outlined above focus on improving understanding of
1005 natural climatic variations, the processes behind these, and possible future changes.
1006 These research areas require urgent investigation as it is clear that there is still a lot
1007 we do not understand with respect to historical climate patterns and causal processes
1008 in the MDB – and even less is known about the future.

1009

1010 **Acknowledgements**

1011 The authors would like to thank Jason Alexandra and the Murray-Darling
1012 Basin Authority for commissioning the reports that formed the basis for this paper and
1013 Stewart Allen for assistance in preparing Figure 4. AG and DK are supported by the
1014 Australian Research Council through the Discovery Projects funding scheme (project
1015 FF0668679).

1016

1017

- 1018

- 1054 Cai, W. and T. Cowan (2008), Dynamics of late autumn rainfall reduction over
1055 southeastern Australia, *Geophys. Res. Lett.*, *35*, L09708, doi:
1056 10.1029/2008GL033727.
- 1057 Cai, W. and T. Cowan (2009), La Niña Modoki impacts Australia autumn rainfall
1058 variability, *Geophys. Res. Lett.*, *36*, L12805, doi:10.1029/2009GL037885.
- 1059 Chambers, D. P., B. D. Tapley, and R. H. Stewart (1999), Anomalous warming in the
1060 Indian Ocean coincident with El Niño, *J. Geophys. Res.*, *104*, 3035-3047.
- 1061 Chiew, F. H. S., T. C. Piechota, J. A. Dracup, and T. A. McMahon (1998), El Nino-
1062 Southern Oscillation and Australian rainfall, streamflow and drought: Links
1063 and potential for forecasting, *J. Hydrol.*, *204*, 138-149.
- 1064 Chiew, F. H. S., J. Teng, D. Kirono, A. Frost, J. Bathols, J. Vaze, N. Viney, K.
1065 Hennessy, and W. Cai (2008), Climate data for hydrologic scenario modelling
1066 across the Murray-Darling Basin *A report to the Australian Government from*
1067 *the CSIRO Murray-Darling Basin Sustainable Yields Project*, 35pp, CSIRO,
1068 Australia.
- 1069 CSIRO and BoM (2007), Climate change in Australia, *Technical Report*, 141pp,
1070 CSIRO and the Australian Bureau of Meteorology.
- 1071 CSIRO (2008), Water availability in the Murray-Darling Basin, 67pp, CSIRO,
1072 Australia.
- 1073 Dommenget, D. and M. Latif (2001), A cautionary note on the interpretation of EOFs,
1074 *J. Clim.*, *15*, 216-225.
- 1075 Dommenget, D. (2007), Evaluating EOF modes against a stochastic null hypothesis,
1076 *Clim. Dynam.*, *28*, 517-531.
- 1077 Dommenget, D. and M. Jansen (2009), Predictions of Indian Ocean SST indices with
1078 a simple statistical model: a null hypothesis, *J. Clim.*, *22*, 4930-4938.
- 1079 Donohue, R. J., T. R. McVicar, and M. L. Roderick (2010), Assessing the ability of
1080 potential evaporation formulations to capture the dynamics in evaporative
1081 demand within a changing climate, *J. Hydrol.*,
1082 doi:10.1016/j.jhydrol.2010.03.020.
- 1083 Draper, C. S. and G. Mills (2008), The Atmospheric Water Balance over the semiarid
1084 Murray-Darling River Basin, *J. Hydrometeorology*, *9*, 521-534.
- 1085 Drosowsky, W. (1993), Potential predictability of winter rainfall over southern and
1086 eastern Australian using Indian Ocean sea-surface temperature anomalies,
1087 *Aust. Met. Mag.*, *42*, 1-6.
- 1088 Drosowsky, W. and L. E. Chambers (2001), Near-global sea surface temperature
1089 anomalies as predictors of Australian seasonal rainfall, *J. Clim.*, *14*, 1677-
1090 1687.

- 1091 Drosowsky, W. (2005), The latitude of the subtropical ridge over eastern Australia:
1092 The L index revisited, *Int. J. Climatol.*, 25, 1291-1299.
- 1093 Drost, F. and M. H. England (2008), Twentieth century trends in moisture advection
1094 over Australia, *Meteorol. Atmos. Phys.*, 100, 243-256.
- 1095 Fischer, A. S., P. Terray, E. Guilyardi, S. Gualdi, and P. Delecluse (2005), Two
1096 independent triggers for the Indian Ocean Dipole/Zonal Mode in a coupled
1097 GCM, *J. Clim.*, 18, 3428-3449.
- 1098 Folland, C. K., D. Parker, A. Colman, and R. Washington (1999), Large scale modes
1099 of ocean surface temperature since the late nineteenth century, in *Beyond El*
1100 *Niño: Decadal and interdecadal climate variability*, edited by A. Navarra, p.
1101 374pp, Springer, Berlin.
- 1102 Folland, C. K., J. A. Renwick, M. J. Salinger, and A. B. Mullan (2002), Relative
1103 influences of the Interdecadal Pacific Oscillation and ENSO on the South
1104 Pacific Convergence Zone, *Geophys. Res. Lett.*, 29, 1643,
1105 doi:10.1029/2001GL014201.
- 1106 Franks, S. W. (2002), Assessing hydrological change: deterministic general
1107 circulation models or spurious solar correlation?, *Hydrological Processes*, 16,
1108 559-564.
- 1109 Frederiksen, C. S., J. S. Frederiksen, J. M. Sisson, and S. L. Osbrough (2011),
1110 Australian winter circulation and rainfall changes and projections,
1111 *International Journal of Climate Change Strategies and Management*, 3, 170-
1112 188.
- 1113 Gallant, A. J. E. and D. J. Karoly (2009), The atypical influence of the 2007 La Niña
1114 on rainfall and temperature in southeastern Australia, *Geophys. Res. Lett.*, 36,
1115 L14707, doi:10.1029/2009GL039026.
- 1116 Gallant, A. J. E. and D. J. Karoly (2010), A combined climate extremes index for the
1117 Australian region, *J. Clim.*, 23, 6153-6165.
- 1118 Gallant, A. J. E. and J. Gergis (2011), An experimental streamflow reconstruction for
1119 the River Murray, Australia, 1783-1988, *Water Resour. Res.*, 47, W00G04,
1120 doi:10.1029/2010WR009832.
- 1121 Gergis, J., A. J. E. Gallant, K. Braganza, R. D'Arrigo, K. Allen, L. Cullen, P.
1122 Grierson, I. Goodwin, and S. McGregor (2011), On the long-term context of
1123 the 1997-2009 'Big Dry' in south-eastern Australia: insights from a 206-year
1124 multi-proxy rainfall reconstruction, *Climatic Change*, doi: 10.1007/s10584-
1125 011-0263-x.
- 1126 Gillett, N. P., T. D. Kell, and P. D. Jones (2006), Regional climate impacts of the
1127 Southern Annular Mode, *Geophys. Res. Lett.*, 33, L23704,
1128 doi:10.1029/2006GL027721.
- 1129 Hendon, H. H. and B. Liebmann (1990), The intraseasonal (30-50 day) oscillation of
1130 the Australian summer monsoon, *J. Atmos. Sci.*, 47, 2909-2924.

- 1131 Hendon, H. H., D. W. J. Thompson, and M. C. Wheeler (2007), Australian rainfall
1132 and surface temperature variations associated with the Southern Hemisphere
1133 Annular Mode, *J. Climate*, 20, 2452-2467.
- 1134 IPCC (2007), *Climate Change 2007: Impacts, Adaptation and Vulnerability.*
1135 *Contribution of Working Group II to the Fourth Assessment Report of the*
1136 *Intergovernmental Panel on Climate Change*, 976pp. Cambridge University
1137 Press, Cambridge, UK.
- 1138 Jones, D. A., W. Wang, and R. Fawcett (2009a), High-quality spatial climate data-sets
1139 for Australia, *Aust. Met. Ocean. Journal*, 58, 233-248.
- 1140 Jones, J. M., R. L. Fogg, M. Widmann, G. J. Marshall, P. D. Jones, and V. M. (2009b),
1141 Historical SAM variability. Part I: Century Length Seasonal Reconstructions,
1142 *J. Clim.*, 22, 5319-5345, doi: 10.1175/2009JCLI2785.1.
- 1143 Karoly, D. J. (1989), Southern Hemisphere circulation features associated with El
1144 Niño-Southern Oscillation events, *J. Clim.*, 2, 1239-1252.
- 1145 Karoly, D. J. (1990), The role of transient eddies in low-frequency zonal variations of
1146 the Southern Hemisphere circulation, *Tellus*, 42A, 41-50.
- 1147 Karoly, D. J. and K. Braganza (2005), A new approach to detection of anthropogenic
1148 temperature changes in the Australian region, *Meteorol. Atmos. Phys.*, 89, 57-
1149 67.
- 1150 Kestin, T. S., D. J. Karoly, and J. I. Yano (1998), Time-frequency variability of
1151 ENSO and stochastic simulations, *J. Climate*, 11, 2258-2272.
- 1152 Kiem, A. S. and S. W. Franks (2001), On the identification of ENSO-induced rainfall
1153 and runoff variability: a comparison of methods and indices, *Hydrolog. Sci. J.*,
1154 46, 715-727.
- 1155 Kiem, A. S., S. W. Franks, and G. Kuczera (2003), Multi-decadal variability of flood
1156 risk, *Geophys. Res. Lett.*, 30, 1035, doi: 10.1029/2002GL015992.
- 1157 Kiem, A. S. and S. W. Franks (2004), Multi-decadal variability of drought risk,
1158 eastern Australia, *Hydrological Processes*, 18, 2039-2050.
- 1159 Kiem, A. S. and D. C. Verdon-Kidd (2009), Climatic drivers of Victorian streamflow:
1160 Is ENSO the dominant influence?, *Australian Journal of Water Resources*, 13,
1161 17-30.
- 1162 Kiem, A. S. and D. C. Verdon-Kidd (2010), Towards understanding hydroclimatic
1163 change in Victoria, Australia - preliminary insights into the 'Big Dry', *Hydrol.*
1164 *and Earth Syst. Sci.*, 14, 433-445.
- 1165 Koster, R. D., P. A. Dirmeyer, Z. C. Guo, G. Bonan, E. Chan, P. Cox, C. T. Gordon,
1166 S. Kanae, E. Kowalczyk, P. J. Lawrence, C. Liu, C. H. Lu, S. Malyshev, B.
1167 McAvaney, K. Mitchell, D. Mocko, T. Oki, K. Oleson, A. Pitman, Y. C. Sud,
1168 C. M. Taylor, D. Verseghy, R. Vasic, Y. K. Xue, and T. Yamada (2004),

- 1169 Regions of strong coupling between soil moisture and precipitation, *Science*,
1170 305, 1138-1140.
- 1171 Larkin, N. K. and D. E. Harrison (2005), Global seasonal temperature and
1172 precipitation anomalies during El Niño autumn and winter, *Geophys. Res.*
1173 *Lett.*, 32, L16705, doi: 10.1029/2005GL037786.
- 1174 Larsen, S. H. and N. Nicholls (2009), Southern Australian rainfall and the subtropical
1175 ridge: Variations, interrelationships, and trends, *Geophys. Res. Lett.*, 36,
1176 doi:10.1029/2009GL037786.
- 1177 Lavery, B., A. Kariko, and N. Nicholls (1992), A historical rainfall data set for
1178 Australia, *Aust. Met. Mag.*, 40, 33-39.
- 1179 Lee, T. and M. J. McPhaden (2010), Increasing intensity of El Niño in the central-
1180 equatorial Pacific, *Geophys. Res. Lett.*, 37, L14603,
1181 doi:10.1029/2010GL044007.
- 1182 Lough, J. M. (2007), Tropical river flow and rainfall reconstructions from coral
1183 luminescence: Great Barrier Reef, Australia, *Paleoceanography*, 22, PA2218,
1184 doi: 10.1029/2006PA001377.
- 1185 Maheshwari, B., K. Walker, and T. McMahon (1995), Effects of regulation on the
1186 flow regime of the River Murray, Australia, *Regul. Rivers: Resour. Manage.*,
1187 10, 15-38.
- 1188 Mantua, N. J., S. R. Hare, Y. Zhang, J. M. Wallace, and R. C. Francis (1997), A
1189 Pacific interdecadal climate oscillation with impacts on salmon production,
1190 *Bulletin of the American Meteorological Society*, 78, 1069-1079.
- 1191 Mantua, N. J. and S. R. Hare (2002), The Pacific Decadal Oscillation, *J.*
1192 *Oceanography*, 58, 35-44.
- 1193 Marshall, G. J. (2003), Trends in the Southern Annular Mode from observations and
1194 reanalyses, *J. Climate*, 16, 4134-4143.
- 1195 McBride, J. L. and N. Nicholls (1983), Seasonal relationships between Australian
1196 rainfall and the southern oscillation, *Mon. Weath. Rev.*, 111, 1998-2004.
- 1197 McIntosh, P. C., M. J. Pook, J. S. Risbey, S. N. Lisson, and M. Rebbeck (2007),
1198 Seasonal climate forecasts for agriculture: Towards better understanding and
1199 value, *Field Crops Research*, 104, 130-138.
- 1200 Meehl, G. A., H. Y. Teng, and G. Branstator (2006), Future changes of El Niño in two
1201 global coupled climate models, *Clim. Dynam.*, 26, 549-566.
- 1202 Meneghini, B., I. Simmonds, and I. N. Smith (2007), Association between Australian
1203 rainfall and the Southern Annular Mode, *Int. J. Climatol.*, 27, 109-121.
- 1204 Meyers, G. A., P. C. McIntosh, L. Pigot, and M. J. Pook (2007), The years of El Niño,
1205 La Niña, and interactions with the tropical Indian Ocean, *J. Climate*, 20, 2872-
1206 2880.

- 1207 Murphy, B. F. and B. Timbal (2008), A review of recent climate variability and
1208 climate change in southeastern Australia, *Int. J. Climatol.*, 28, 859-879.
- 1209 Nicholls, N. (1984), The Southern Oscillation and Indonesian sea surface temperature,
1210 *Mon. Weath. Rev.*, 112, 424-432.
- 1211 Nicholls, N. (1988), El Niño - Southern Oscillation and rainfall variability, *J. Clim.*, 1,
1212 418-421.
- 1213 Nicholls, N. (1989), Sea surface temperatures and Australian winter rainfall, *J. Clim.*,
1214 2, 965-973.
- 1215 Nicholls, N. and A. Kariko (1993), East Australian rainfall events: Interannual
1216 variations, trends, and relationships with the Southern Oscillation, *J. Climate*,
1217 6, 1141-1152.
- 1218 Nicholls, N. (2004), The changing nature of Australian droughts, *Climatic Change*,
1219 63, 323-336.
- 1220 Nicholls, N. (2009), Local and remote causes of the southern Australian autumn-
1221 winter rainfall decline, 1958-2007, *Climate Dynamics*, 11, doi:
1222 10.1007/s00382-009-0527-6.
- 1223 Pezza, A. B., I. Simmonds, and J. A. Renwick (2007), Southern Hemisphere cyclones
1224 and anticyclones: Recent trends and links with decadal variability in the
1225 Pacific Ocean, *Int. J. Climatol.*, 27, 1403-1419.
- 1226 Pezza, A. B., T. Durrant, and I. Simmonds (2008), Southern Hemisphere synoptic
1227 behavior in extreme phases of SAM, ENSO, sea ice extent, and southern
1228 Australia rainfall, *J. Climate*, 21, 5566-5584.
- 1229 Pittock, A. B. (1975), Climate change and the patterns of variation in Australian
1230 rainfall, *Search*, 6, 498-504.
- 1231 Pook, M. J., P. C. McIntosh, and G. A. Meyers (2006), The synoptic decomposition of
1232 cool-season rainfall in the southeastern Australian cropping region, *J. Appl.*
1233 *Met. Clim.*, 45, 1156-1170.
- 1234 Power, S., F. Tseitkin, S. Torok, B. Lavery, R. Dahni, and B. McAvaney (1998),
1235 Australian temperature, Australian rainfall and the Southern Oscillation, 1910-
1236 1992: coherent variability and recent changes, *Aust. Met. Mag.*, 47, 85-101.
- 1237 Power, S., T. Casey, C. K. Folland, A. Colman, and V. Mehta (1999a), Interdecadal
1238 modulation of the impact of ENSO on Australia, *Climate Dynamics*, 15, 319-
1239 324.
- 1240 Power, S., F. Tseitkin, V. Mehta, B. Lavery, S. Torok, and N. Holbrook (1999b),
1241 Decadal climate variability in Australia during the twentieth century, *Int. J.*
1242 *Climatol.*, 19, 169-184.

- 1243 Qi, L., L. M. Leslie, and S. X. Zhao (1999), Cut-off low pressure systems over
1244 southern Australia: Climatology and case study, *Int. J. Climatol.*, *19*, 1633-
1245 1649.
- 1246 Quinn, W. H., D. O. Zopf, K. S. Short, and R. T. W. Kuo Yang (1978), Historical
1247 trends and statistics of the Southern Oscillation, El Niño and Indonesian
1248 droughts, *Fish. Bull.*, *76*, 663-678.
- 1249 Rayner, N. A., D. E. Parker, E. B. Horton, C. K. Folland, L. V. Alexander, D. P.
1250 Rowell, E. C. Kent, and A. Kaplan (2003), Global analyses of sea surface
1251 temperature, sea ice, and night marine air temperature since the late nineteenth
1252 century, *J. Geophys. Res.*, *108*, 4407, doi: 10.1029/2002JD002670.
- 1253 Risbey, J. S., M. J. Pook, P. C. McIntosh, C. C. Ummenhofer, and G. A. Meyers
1254 (2008), Characteristics and variability of synoptic features associated with
1255 cool season rainfall in southeastern Australia, *Int. J. Climatol.*, doi:
1256 10.1002/joc.1775.
- 1257 Risbey, J. S., M. J. Pook, P. C. McIntosh, M. C. Wheeler, and H. H. Hendon (2009),
1258 On the remote drivers of rainfall variability in Australia, *Mon. Weath. Rev.*,
1259 *137*, 3233-3253, doi: 10.1175/2009MWR2861.1.
- 1260 Ropelewski, C. F. and M. S. Halpert (1987), Global and regional scale precipitation
1261 patterns associated with the El Niño/Southern Oscillation, *Mon. Weath. Rev.*,
1262 *115*, 1606-1626.
- 1263 Saji, N. H., B. N. Goswami, P. N. Vinayachandran, and T. Yamagata (1999), A dipole
1264 mode in the tropical Indian Ocean, *Nature*, *401*, 360-363.
- 1265 Silvestri, G. and C. Vera (2009), Nonstationary impacts of the Southern Annular
1266 Mode on Southern Hemisphere climate, *J. Clim.*, *22*, 6142-6148.
- 1267 Simmonds, I. (1990), A modelling study of winter circulation and precipitation
1268 anomalies associated with Australian region ocean temperatures, *Aust. Met.*
1269 *Mag.*, *38*, 151 - 161.
- 1270 Smith, I. N. and B. Timbal (2010), Links between tropical indices and southern
1271 Australian rainfall, *Int. J. Climatol.*, doi: 10.1002/joc.2251.
- 1272 Stone, R. and A. Auliciems (1992), SOI phase relationships with rainfall in eastern
1273 Australia, *Int. J. Climatol.*, *12*, 625-636.
- 1274 Stone, R. C., G. L. Hammer, and T. Marcussen (1996), Prediction of global rainfall
1275 probabilities using phases of the Southern Oscillation Index, *Nature*, *384*, 252-
1276 255.
- 1277 Sturman, A. and N. Tapper (2005), *The weather and climate of Australia and New*
1278 *Zealand*, 2nd edition ed., 541pp. Oxford University Press, Melbourne.
- 1279 Sun, F. B., M. L. Roderick, W. H. Lim, and G. D. Farquhar (2011), Hydroclimatic
1280 projections for the Murray-Darling Basin based on an ensemble derived from

- 1281 Intergovernmental Panel on Climate Change AR4 climate models, *Water*
1282 *Resources Research*, 47(W00G02), 10.1029/2010WR009829.
- 1283 Taschetto, A. S. and M. H. England (2009), El Niño Modoki impacts on Australian
1284 rainfall, *J. Climate*, 22, 3167-3174.
- 1285 Taschetto, A. S., C. C. Ummenhofer, A. Sen Gupta, and M. H. England (2009), Effect
1286 of anomalous warming in the central Pacific on the Australian monsoon,
1287 *Geophys. Res. Lett.*, 36, L12704, doi: 10.1029/2009GL038416.
- 1288 Thompson, D. W. J. and J. M. Wallace (2000), Annular modes in the extratropical
1289 circulation, part I: month-to-month variability, *J. Clim.*, 13, 1000-1016.
- 1290 Thompson, D. W. J. and S. Solomon (2002), Interpretation of recent southern
1291 hemisphere climate change, *Science*, 296, 895-899.
- 1292 Timbal, B., S. Power, R. Colman, J. Viviani, and S. Lirola (2002), Does soil moisture
1293 influence climate variability and predictability over Australia?, *J. Clim.*, 15,
1294 1230-1238.
- 1295 Timbal, B. and B. F. Murphy (2007), Observed climate change in the south-east of
1296 Australia and its relation to large-scale modes of variability, *Bureau of*
1297 *Meteorology Research Centre Research Letter No. 6*, 6pp.
- 1298 Timbal, B., B. F. Murphy, K. Braganza, H. H. Hendon, M. C. Wheeler, and C. Rakich
1299 (2007), Compare documented climate changes with those attributable to
1300 specific causes *Project 1.1.2*, 19, South East Australian Climate Initiative,
1301 Centre for Australian Weather and Climate Research, Melbourne, Australia.
- 1302 Trenberth, K. E. and K. C. Mo (1985), Blocking in the Southern Hemisphere, *Mon.*
1303 *Weath. Rev.*, 113, 3-21.
- 1304 Troup, A. J. (1965), The Southern Oscillation, *Quart. J. R. Met. Soc.*, 91, 490-506.
- 1305 Ummenhofer, C. C., A. Sen Gupta, A. S. Taschetto, and M. H. England (2009a),
1306 Modulation of Australian precipitation by meridional gradients in east Indian
1307 Ocean sea surface temperatures, *J. Clim.*, 22, 5597-5610.
- 1308 Ummenhofer, C. C., M. H. England, P. C. McIntosh, G. A. Meyers, M. J. Pook, J. S.
1309 Risbey, A. Sen Gupta, and A. S. Taschetto (2009b), What causes southeast
1310 Australia's worst droughts?, *Geophys. Res. Lett.*, 36, L04706,
1311 doi:10.1029/2008GL036801.
- 1312 Verdon, D. C., A. S. Kiem, and S. W. Franks (2004a), Multi-decadal variability of
1313 forest fire risk - Eastern Australia, *Int. J. Wildland Fire*, 13, 165-171.
- 1314 Verdon, D. C., A. M. Wyatt, A. S. Kiem, and S. W. Franks (2004b), Multi-decadal
1315 variability of rainfall and streamflow - Eastern Australia, *Water Resour. Res.*,
1316 40, W10201, doi: 10.1029/2004WR003234.

- 1317 Verdon, D. C. and S. W. Franks (2005), Indian Ocean sea surface temperature
1318 variability and winter rainfall: eastern Australia, *Water Resour. Res.*, *41*,
1319 W09413, doi:10.1029/2004WR003845.
- 1320 Verdon, D. C. and S. W. Franks (2006), Long-term behaviour of ENSO: Interactions
1321 with the PDO over the past 400 years inferred from paleoclimate records,
1322 *Geophys. Res. Lett.*, *33*, L06712, doi:10.1029/2005GL025052.
- 1323 Verdon-Kidd, D. C. and A. S. Kiem (2009a), On the relationship between large-scale
1324 climate modes and regional synoptic patterns that drive Victorian rainfall,
1325 *Hydrol. and Earth Syst. Sci.*, *13*, 467-479.
- 1326 Verdon-Kidd, D. C. and A. S. Kiem (2009b), Nature and causes of protracted
1327 droughts in southeast Australia: Comparison between the Federation, WWII,
1328 and Big Dry droughts, *Geophys. Res. Lett.*, *36*, L22707,
1329 doi:10.1029/2009GL041067.
- 1330 Wang, G. and H. H. Hendon (2007), Sensitivity of Australian rainfall to inter-El Nino
1331 variations, *J. Climate*, *20*, 4211-4226.
- 1332 Webster, P. J., A. M. Moore, J. P. Loschnigg, and R. R. Leben (1999), Coupled
1333 ocean-atmosphere dynamics in the Indian Ocean during 1997-98, *Nature*, *401*,
1334 356-360.
- 1335 Wheeler, M. C., H. H. Hendon, S. Cleland, H. Meinke, and A. Donald (2009),
1336 Impacts of the Madden-Julian Oscillation on Australian rainfall and
1337 circulation, *J. Climate*, *22*, 1482-1498.
- 1338 White, W. B., G. McKeon, and J. Syktus (2003), Australian drought: The interference
1339 of multi-spectral global standing modes and travelling waves, *Int. J. Climatol.*,
1340 *23*, 631-662.
- 1341 White, W. B., A. Gershunov, J. L. Annis, G. McKeon, and J. Syktus (2004),
1342 Forecasting Australian drought using Southern Hemisphere modes of seas-
1343 surface temperature variability, *Int. J. Climatol.*, *24*, 1911-1927.
- 1344 Williams, A. A. J. and R. C. Stone (2009), An assessment of relationships between
1345 the Australian subtropical ridge, rainfall variability, and high-latitude
1346 circulation patterns, *Int. J. Climatol.*, *29*, 691-709.
- 1347 Wooldridge, S. A., S. W. Franks, and J. D. Kalma (2001), Hydrological implications
1348 of the Southern Oscillation: variability of the rainfall-runoff relationship,
1349 *Hydrolog. Sci. J.*, *46*, 73-88.
- 1350 Wright, W. J. (1989), A synoptic climatological classification of winter precipitation
1351 in Victoria, *Aust. Met. Mag.*, *37*, 217-229.
- 1352 Wright, W. J. (1997), Tropical-extratropical cloudbands and Australian rainfall: 1.
1353 Climatology, *Int. J. Climatol.*, *17*, 807-829.
- 1354 Zhang, Y., J. M. Wallace, and D. S. Battisti (1997), ENSO-like interdecadal
1355 variability: 1900-93, *J. Clim.*, *10*, 1004-1020.

1356

1357

1358

FIGURE CAPTIONS

Figure 1. The Murray-Darling Basin (dashed outline) overlaid on mean annual January – December (1900– 2010) observed rainfall (mm), from the Australian Bureau of Meteorology Australian Water Availability Project rainfall grids [Jones *et al.*, 2009a]. Adapted from Draper and Mills [2008].

Figure 2. Area-average annual (January – December) rainfall (thin grey line) and decadal mean rainfall (thick black line) for the Murray-Darling Basin from 1900 to 2010, generated from the Australian Water Availability Project rainfall grids [Jones *et al.*, 2009a]. The dashed line indicates the mean annual rainfall total over the 1900 – 2010 mean (471 mm).

Figure 3. The 13-year June 1997 to May 2009 rainfall totals shown as deciles compared to all other 13-year June to May periods from June 1900 to January 2009. Figure provided by the Australian Bureau of Meteorology.

Figure 4. The key weather systems that affect the Murray-Darling Basin during the austral (a) summer (DJF) and (b) winter (JJA). The southern half of the Basin is primarily affected by extra-tropical systems and receives the majority of its annual rainfall during the cooler months (May–October). The northern half of the Basin is primarily affected by tropical systems and interactions between tropical and extra-tropical systems and receives the majority of its annual rainfall during the warmer months (November–April). The systems that tend to suppress rainfall are shown in red.

Figure 5. The squares represent the difference in the 6-monthly (April–September) mean number of heavy rain days (defined as days with over 25 mm of rainfall)

between years experiencing neutral and extreme phases of ENSO, SAM and Indian Ocean SST variations. The mean number of rain days during years in the positive (top row) and negative (bottom row) phases of ENSO (left column), SAM (centre column) and eastern Indian Ocean SSTs (right column) are shown. Blue indicates that a station has more, and red that a station has less heavy rain days than in neutral years. A solid square indicates this difference is significant at the 95% level based on a confidence interval generated from 1000 bootstrap replicates of neutral years.

Figure 6. Running 30-year correlations between pairs of seasonal indices representing the drivers of inter-annual climate variability in the MDB. SAM and STR intensity (solid black line), SAM and STR latitude (dashed black line), SAM and ENSO (solid yellow line), ENSO and IOD (solid blue line), ENSO and the eastern pole of the IOD (dashed blue line), ENSO and STR intensity (solid red line), and ENSO and STR latitude (dashed red line) are shown. A t-distribution with a sample size of 30 years was used to estimate the bounds of statistical significance and is indicated by the thin dashed lines ($t = \pm 0.35$).

Figure 7. Composite mean percentage winter (June–August) rainfall anomalies in the MDB during co-occurring phases of the SAM and ENSO from 1905–2004. A positive or negative phase of SAM and ENSO was defined when the standardized anomalies (relative to 1905–2004) of each index exceeded ± 0.5 standard deviations. Red colours indicate rainfall deficits and blue, rainfall surplus. The number, n , in each panel indicates the number of years from which the composite was computed, this is, the number of years in which the particular phases of ENSO and SAM co-occurred. Rainfall data is from the AWAP high-quality Australian rainfall grids [Jones *et al.*, 2009a].

Table 1. The seasonality of the inter-annual and longer hydroclimate processes for the Murray-Darling Basin is identified. The black circles indicate the months in which previous studies (see Section 3) have reported an influence of the process stated in the left-half column on the Murray-Darling Basin's climate. The months shaded in orange (March, April, May, June) are those that experienced large and persistent rainfall deficits during the Big Dry (c. 1997–2010).

	J	F	M	A	M	J	J	A	S	O	N	D
<i>Inter-annual processes</i>												
El Niño – Southern Oscillation	●	●	●			●	●	●	●	●	●	●
Indian Ocean SSTs						●	●	●	●	●	●	
Southern Annular Mode	●	●				●	●	●	●	●	●	●
Sub-Tropical Ridge Intensity				●	●	●	●					
Sub-Tropical Ridge Position	●	●										●
Tropical North Australia SSTs									●	●	●	
ENSO/SAM interactions	●	●	●	●	●	●	●	●	●	●	●	●
<i>Inter-decadal – centennial</i>												
Inter-decadal Pacific Oscillation	●	●				●	●	●	●	●	●	●
Anthropogenic climate change	●	●	●	●	●	●	●	●	●	●	●	●

Table 2. Identifies the characteristics of the Big Dry that are consistent with the typical influences of known climate processes. These include similarities in spatial and temporal features and associated small-scale influences e.g. the influence of an inter-annual process on weather systems. The seven major defining characteristics of the drought identified in Section 5 are stated below the table. A tick indicates that a characteristic feature of the drought is consistent with current understanding of how the processes in the far-left column influence the regional climate, a cross indicates an inconsistency, and a dash indicates that the link between that characteristic and the climate process is unknown.

Characteristic drought feature	1	2	3	4	5	6	7
<i>Inter-annual processes</i>							
El Niño – Southern Oscillation	✓	✗	✓	–	–	–	✗
Indian Ocean SSTs	✓	✗	✓	–	–	–	–
Southern Annular Mode	✓	✗	✓	–	–	✓	–
Sub-Tropical Ridge Intensity	✓	✓	✓	–	–	–	✓
Sub-Tropical Ridge Position	✓	✗	✗	–	–	–	✓
Tropical North Australia SSTs	✓	✗	✓	–	–	–	–
ENSO/SAM interactions	✓	✓	✓	✓	–	✓	–
<i>Inter-decadal – centennial</i>							
Inter-decadal Pacific Oscillation	✓	✗	✓	✓	–	–	–
Anthropogenic climate change	✓	✓	✓	–	–	–	✓
<i>Trends</i>							
Trend in STR intensity	✓	✓	✓	–	–	–	✓
Southerly shift in storm track	✓	✓	✓	–	–	✓	✓
Warmer Indian Ocean SSTs	✓	✗	✓	–	–	–	–

Major defining characteristics of the Big Dry.

¹ Impacts the southern Murray-Darling Basin (south of approximately 33°S)

² Persistent late autumn and early winter (MAMJ) rainfall deficits

³ Occasional winter/spring rainfall deficits

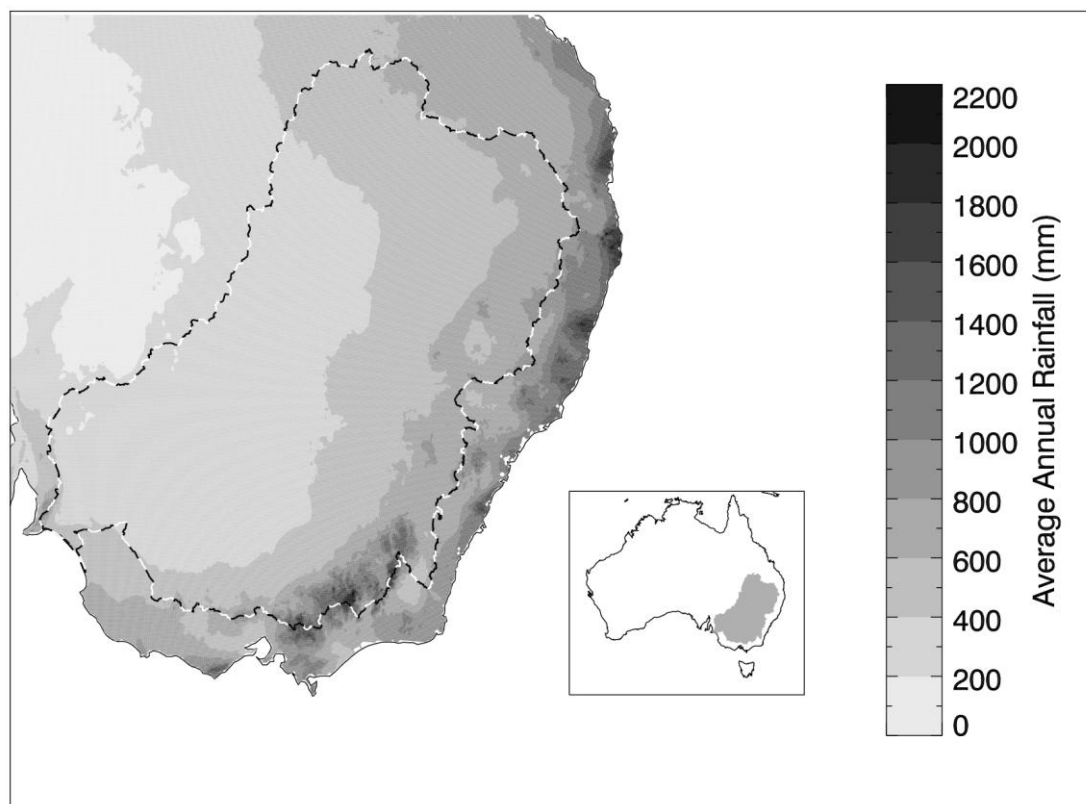
⁴ Lack of high rainfall periods and high one-day rainfall totals

⁵ Reduction in rainfall stemming from cut-off low pressure systems

⁶ Absence of rain-bearing troughs

⁷ Increases in surface pressure

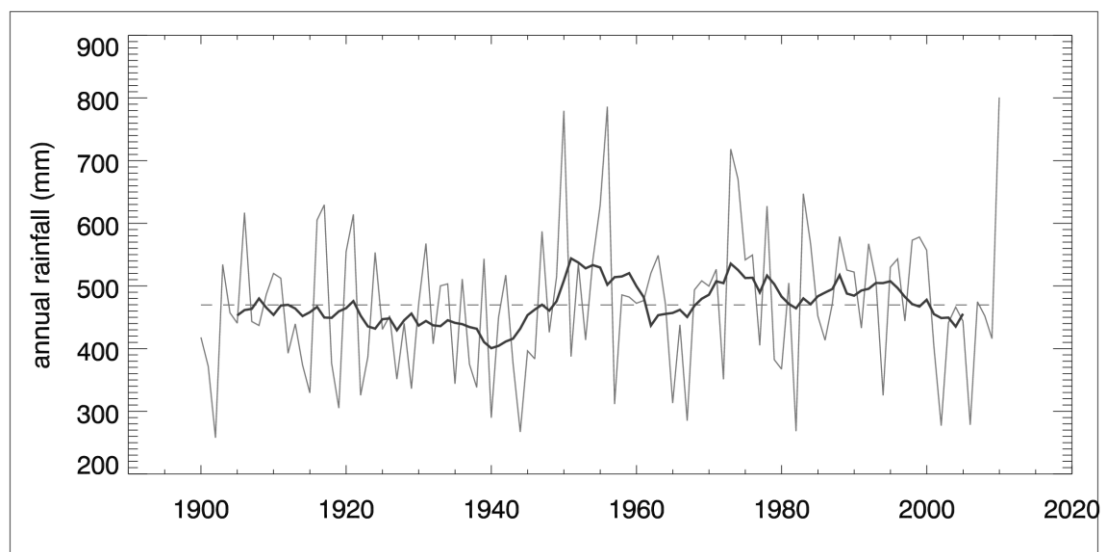
1433 **Figure 1**



1434

1435

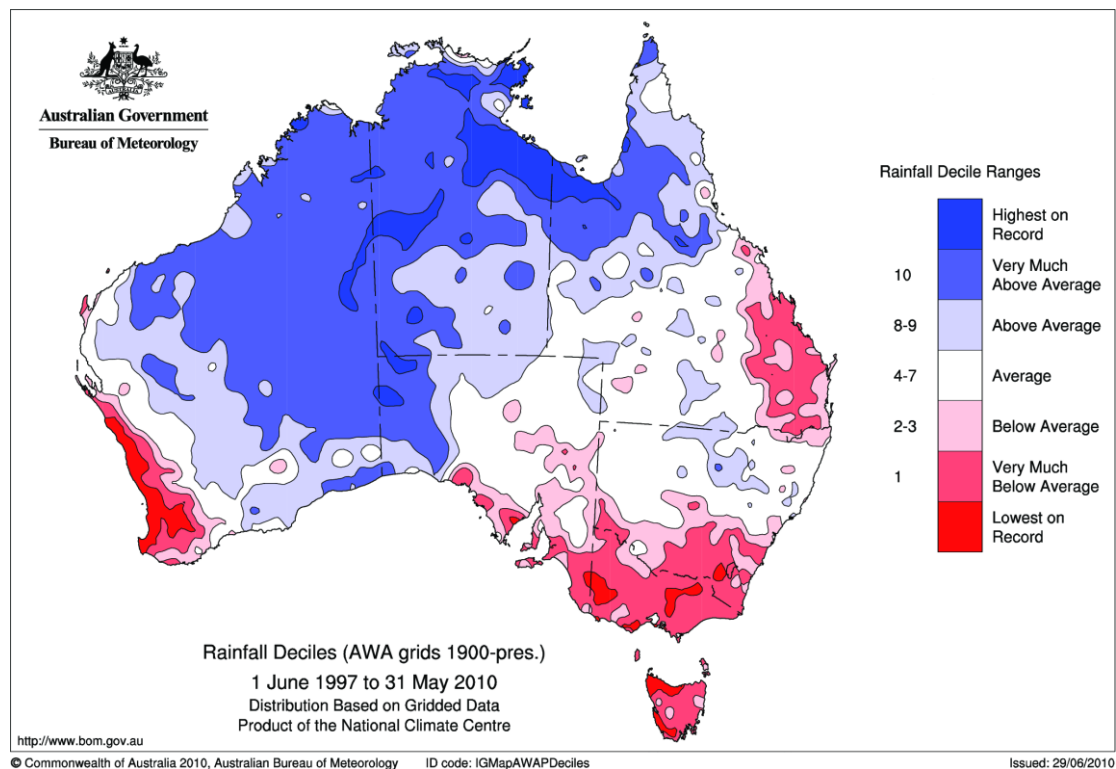
1436 **Figure 2**



1437

1438

1439 **Figure 3**

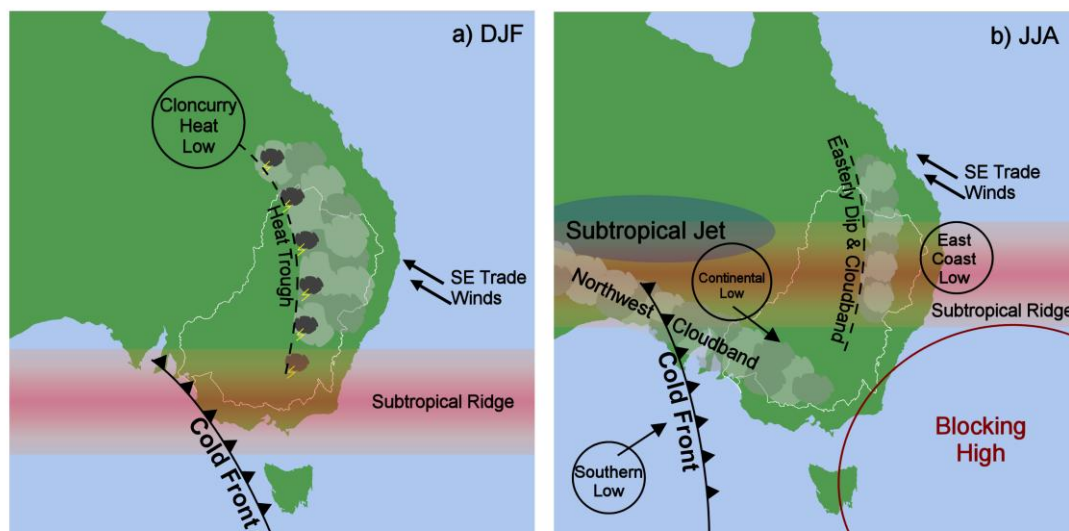


1440

1441

1442

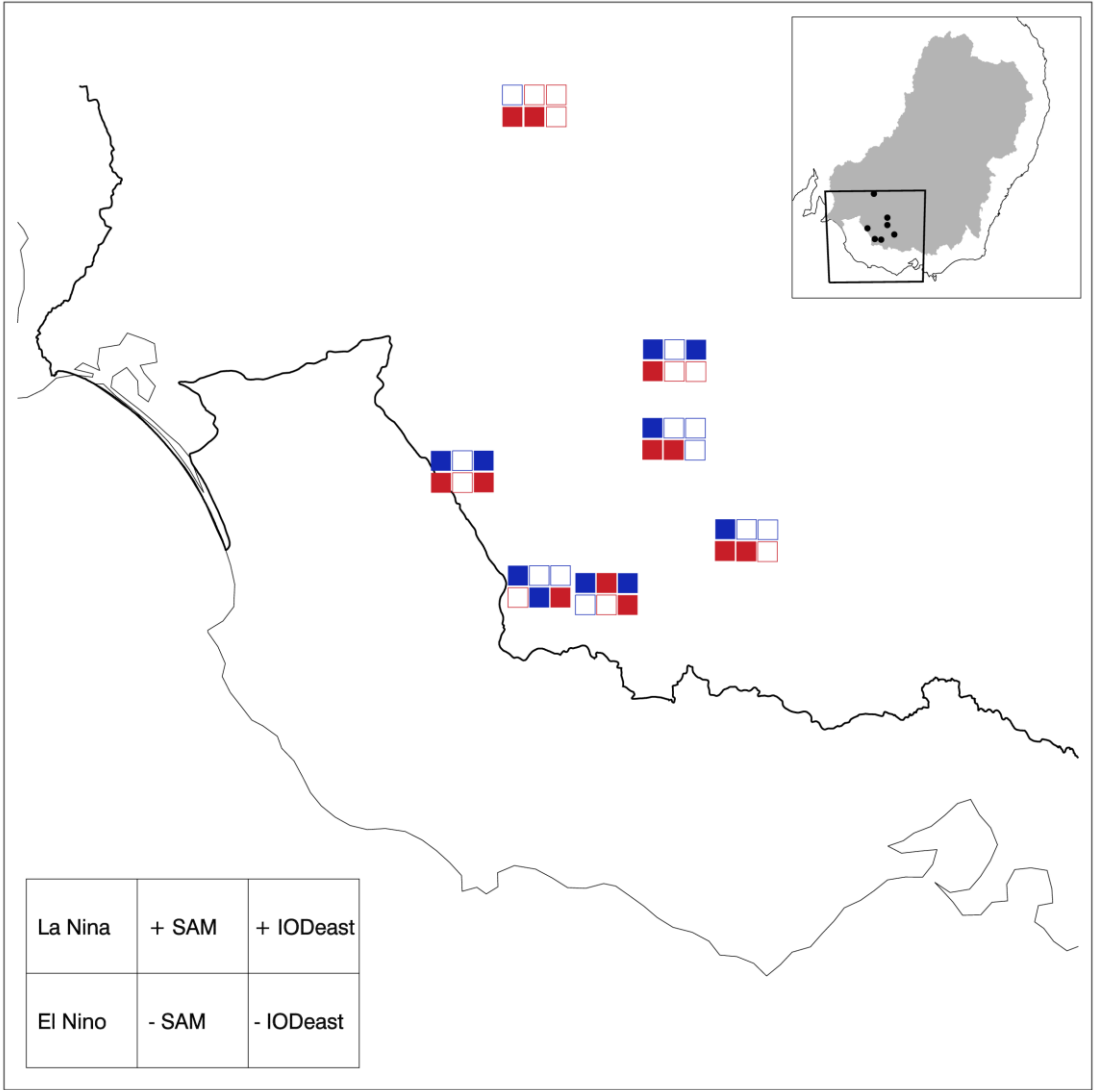
1443 **Figure 4**



1444

1445

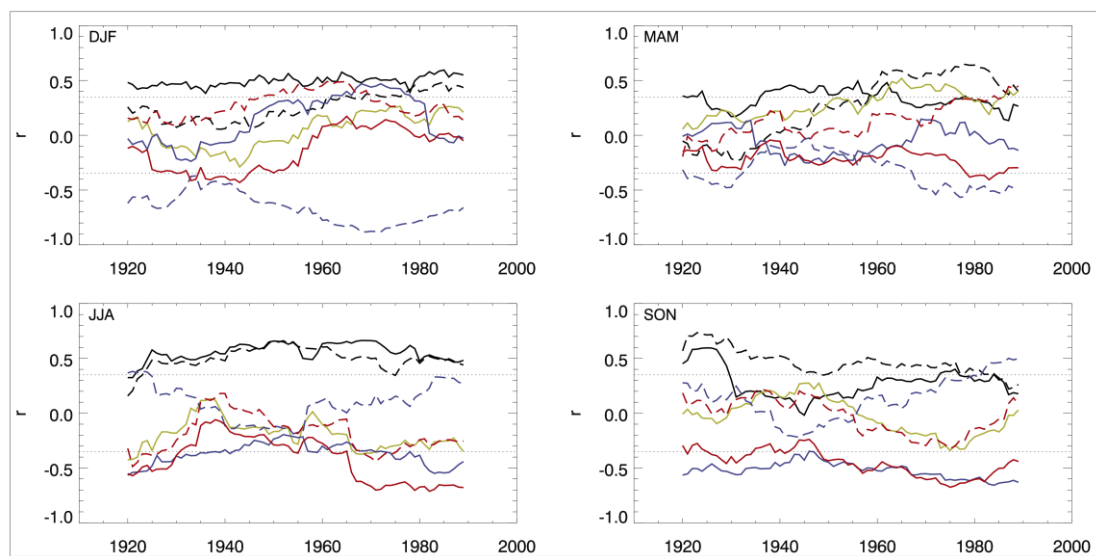
1446 **Figure 5**



1447

1448

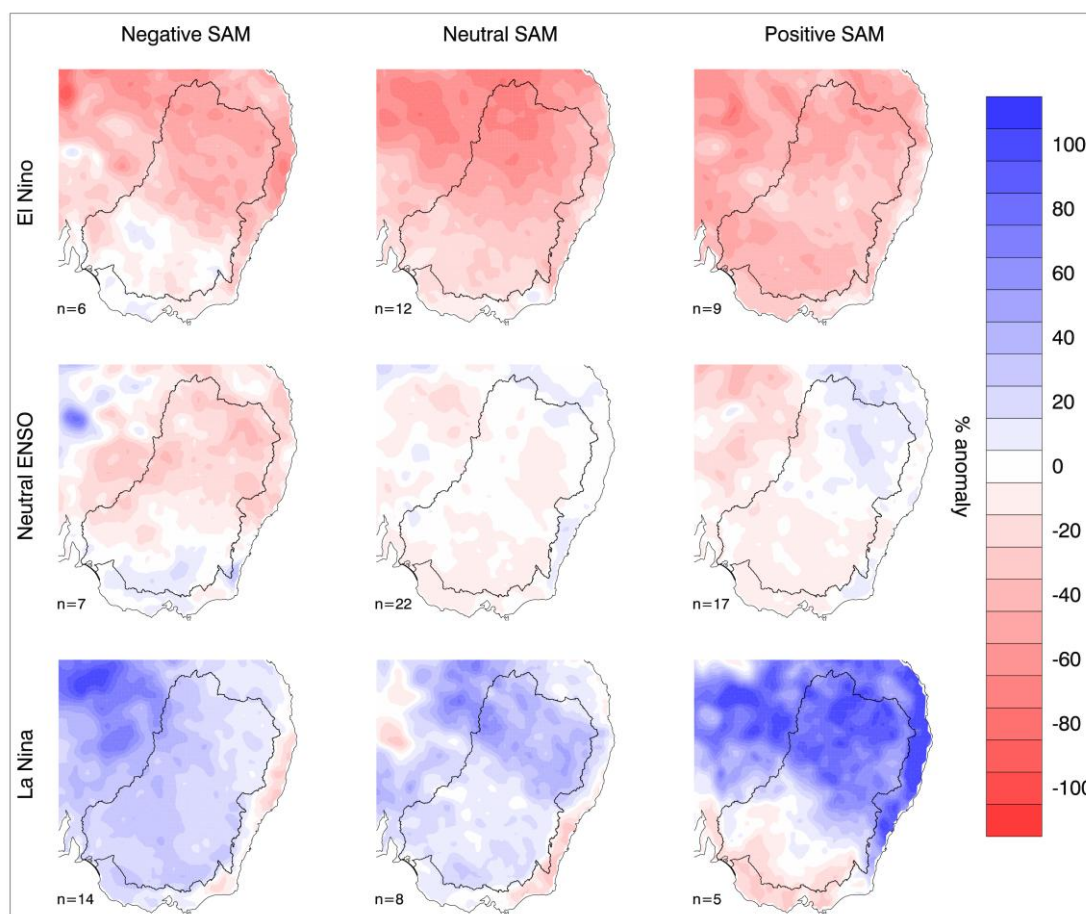
1449 **Figure 6**



1450

1451

1452 **Figure 7**



1453

1454